Feeding the Export Boom: Technological Change and Land Use in Brazil's Beef Industry

Peter O'Brien*
UC Davis

November 1, 2026

PLEASE CLICK HERE FOR THE LATEST VERSION OF THIS PAPER.

Beef is among the most land- and emissions-intensive foods. In Brazil, expanding agricultural production has historically driven deforestation across carbon-rich ecosystems, including the Amazon. Rapid growth in beef exports raises concerns about further land conversion, yet access to foreign markets may also encourage agricultural intensification, or the adoption of technologies that reduce land requirements per unit of output. Because this intensification is difficult to observe, I use satellite imagery and deep learning to build a novel panel of Brazilian feedlots, facilities where cattle are produced in confinement rather than grazing on pasture. I combine this panel with records of processing-plant authorizations to study the effects of Brazil's beef export boom to China. I exploit variation in the timing of plant authorizations and regions' exposure to newly authorized plants and find that greater export exposure substantially increased feedlot entry and total capacity. Holding current beef production fixed, replacing this China-induced intensive production with traditional, grazing-based systems would require approximately 1.29 million additional hectares of pasture. This would put 169 $MtCO_2$ of carbon stocks at risk, an amount greater than one-third of Brazil's annual emissions, underscoring how trade-induced technological change can shape the environmental consequences of agricultural production.

*I thank Katrina Jessoe, James Sayre, and Ishan Nath for their invaluable advice and mentorship throughout this project. All errors are my own.
Contact: paobrien@ucdavis.edu

1 Introduction

Agricultural production and the environment are inextricably linked. Global growth in agricultural exports has raised concerns that trade can increase pressure on land and natural resources in producing regions (Food and Agriculture Organization of the United Nations 2022). These concerns are particularly important for commodities such as beef, which uses approximately 15% of the world's habitable land area for production (Poore and Nemecek 2018). Increased market exposure represents a demand shock to local producers, increasing incentives to expand output and potentially convert previously undeveloped land. However, the environmental effects of trade depend not only on the scale of production, but also on how efficiently goods are produced. Greater export access may also encourage agricultural intensification, as producers adopt technologies that reduce land requirements per unit of output. This "technique effect" could offset some of the land-use pressure associated with expanding production (Copeland and Taylor 2004). Understanding the environmental consequences of agricultural trade therefore requires a better understanding of how export exposure drives the adoption of land-sparing production technologies. This paper examines that relationship and quantifies its implications for land use and associated carbon emissions.

This relationship is particularly relevant for Brazil's beef industry, where pasture expansion accounts for roughly one-quarter of global deforestation since 2001 (Singh and Persson 2026). The conversion of land for pasture in regions such as the Amazon releases stored carbon and threatens ecosystems that play a crucial role in climate change mitigation through their role as carbon sinks. At the same time, Brazil has become an increasingly important supplier to global agricultural markets. Its share of world agricultural exports rose from 4.3% in 2000 to 9.7% in 2024, and it is now the world's largest beef exporter (World Trade Organization 2026). This growth raises questions about how export demand will shape land pressure in this region. I therefore ask: Does access to a large export market induce the adoption of more intensive beef production? If so, how does that technological response affect the amount and spatial distribution of grazing land required to produce Brazilian beef?

I address these questions using Brazil's beef export boom to China, which has become the largest destination for Brazilian beef exports. Access to the Chinese market is regulated at the processing-plant level, as individual facilities must receive bilateral authorization before exporting to China. In addition, cattle destined for the Chinese market are subject to production requirements that differ from those in the domestic market. Using administrative records obtained through information requests to the Brazilian government, I reconstruct the history of these plant-level export authorizations. Because authorizations were granted in staggered waves and cattle-producing regions differ in their proximity

to authorized plants, this process generated substantial spatial and temporal variation in exposure to a large, foreign market. I use this structured expansion of access to study how export exposure drives agricultural intensification in my setting.

Measuring this technological response to export exposure is challenging, as conventional measures of agricultural productivity, such as output per hectare, capture aggregate changes in efficiency but not the underlying investment decisions that generate these changes. This is particularly true for cattle production, where aggregate, point-in-time measures such as stocking rates (cattle per hectare of pasture) do not reveal how cattle are raised, how quickly they gain weight, or how much time they spend grazing over the production cycle. I focus on one important form of intensification: confined cattle-feeding operations, commonly known as "feedlots," where cattle are fed grain-based diets in confined pens. Feedlot-based production allows cattle to reach marketable weight more quickly, reducing the time they spend grazing, and their well-documented production characteristics allow me to relate the physical footprint of facilities to their production capacity. However, comprehensive data on the location and development of these facilities are unavailable. To address this gap, I construct a novel panel of Brazilian feedlots using deep learning applied to high-resolution satellite imagery to identify facilities and measure their pen area. I then develop a custom approach that draws on methods from structural-break estimation and remote sensing to date their establishment, allowing me to measure where and when intensive finishing capacity developed across Brazil.

Obtaining credible estimates of the effect of export market access on feedlot development faces several challenges. First, plants authorized to export to China are not randomly selected, so regions gaining market access may differ systematically from those without access. I begin by exploiting the staggered timing of authorizations in an event study design, comparing feedlot development in regions exposed to newly authorized plants with regions gaining access later. However, authorization timing may itself be selective, even among candidate plants. I address this by using the institutional structure of the bilateral approval process to define groups of plants within which authorization timing can be treated as plausibly exogenous. Finally, some regions are mechanically more likely to gain exposure because they are located near many candidate plants. I therefore implement a "recentered exposure" design following Borusyak and Hull (2023) that compares realized authorization patterns with counterfactual assignments within these groups, isolating shocks to predicted exposure that are driven solely by uncertainty in the timing of authorizations by Chinese officials.

I first document that feedlot development is geographically concentrated around processing plants connected to the Chinese market. I also show that these plants increasingly source younger, feedlot-finished cattle following authorization, consistent with a broader shift toward intensive production. The event study results provide preliminary evidence

that feedlot entry rises in regions near recently authorized export plants, demonstrating that feedlot concentration near export plants is not merely a reflection of strategic authorization assignment where existing capacity is high. Using the more conservative recentered exposure design, I find that greater export exposure substantially increases both feedlot entry and confined-finishing capacity. My estimates imply that municipalities one standard deviation more exposed to the Chinese market built 3.8 times as many feedlots.

To quantify the land-use implications of this technological response, I use my reduced-form results to estimate the share of current confined-finishing capacity attributable to Chinese market access and evaluate a counterfactual scenario where this additional capacity was never realized. I calibrate beef production parameters informed by industry data and use cattle-movement records to trace the sourcing of cattle through the supply chain and allocate grazing requirements to upstream producing regions. Holding current beef production fixed, these back-of-the-envelope estimates suggest that replacing China-induced feedlot production with traditional pasture-based systems would require approximately 1.29 million additional hectares of grazing land. Allocating this additional land requirement across supplying regions according to observed cattle movements and historical land-conversion patterns implies 169 $MtCO_2$ of potential carbon stock losses.

This paper contributes to the trade-and-environment literature by showing how export market access can change environmental resource use through induced technological change, rather than only through changes in the scale or location of production. Recent work emphasizes how trade reallocates agricultural production across locations with heterogeneous resource endowments and environmental costs (Carleton, Crews, and Nath 2025; Farrokhi, Kang, Pellegrina et al. 2025; Mishra 2025). My paper focuses on a complementary channel. Exposure to international markets can induce producers to adopt technologies that change resource requirements per unit of output. While Shapiro and Walker (2018) attribute most of the decline in pollution intensity in U.S. manufacturing to environmental regulation, I study a setting in which trade itself is a major driver of the technique effect. Because I observe the underlying technological change directly, rather than infer it from changes in resource use per unit of output, I can link trade exposure to a specific change in production technology.

This paper builds on existing work on agricultural supply chains by showing how a downstream shock propagates upstream into production decisions and land use. Recent work examines how environmental policy and export demand propagate through agricultural supply chains, and how these linkages shape the spatial concentration of production (Domínguez-Iino 2025; Sayre 2026; Amodio, Chiovelli, and Frache 2025). I study a complementary margin by asking how a downstream export-demand shock changes the production technology adopted upstream, which in turn shapes the spatial distribution of land requirements. In particular, feedlot finishing changes pasture requirements at

earlier stages of cattle production, potentially far from where feedlots are located. Using cattle movement data, I estimate how these changes in land requirements are distributed across upstream sourcing regions.

The paper also relates to the literature on agricultural production and deforestation in the Brazilian Amazon. Existing work examines how deforestation policies affect forest loss and induce investment and productivity improvements in this sector (Assunção, McMillan, Murphy et al. 2023; Moffette, Skidmore, and Gibbs 2021), and maps the deforestation risk associated with beef export supply chains (zu Ermgassen, Suavet, Biddle et al. 2023). My paper is the first to quantify how export market access can induce intensification in Brazil's cattle sector, showing how market incentives, in addition to conservation policy, can reduce the land required for beef production and potentially ease pressure for expansion along the Amazon frontier.

My work also contributes to the literature on technological change in agriculture. Existing work in the Latin American context highlights how export growth and new agricultural technologies can generate spillovers to the broader economy, potentially leading to structural transformation (Bustos, Caprettini, and Ponticelli 2016; Pellegrina 2022). Beyond agriculture, Bustos (2011) shows how trade liberalization can induce technology upgrading among manufacturing firms. My paper demonstrates an additional channel through which trade exposure can induce technology adoption: an export market premium coupled with sourcing standards that favor more intensive production. In addition, I quantify the environmental implications of this trade-driven upgrading. Finally, this paper contributes to an emerging literature that uses deep learning to construct measures of infrastructure development and economic activity (Dell 2025; Khachiyan, Thomas, Zhou et al. 2022; Marx, Stoker, and Suri 2019). I use object detection to construct a national panel of feedlot openings and physical expansion, providing a direct measure of investment and technological adoption that is not systematically observable in available data.

In the remainder of the paper, I first describe the Brazilian beef supply chain and access to the Chinese market, introduce the data and feedlot detection methodology, and present stylized facts on the expansion of intensive finishing. I then develop the empirical strategy and reduced-form estimates of the response to increased Chinese market exposure, use cattle-movement data to characterize the upstream sourcing network, and combine these estimates in a land-use accounting counterfactual. The final sections quantify the associated environmental implications and discuss the broader implications for trade, technological change, and agricultural land use.

2 Data

2.1 Setting

Brazil has the world's largest commercial cattle herd and is the largest beef exporter, but production has historically relied predominantly on extensive, grazing-based systems. The beef production process can be divided broadly into three stages: breeding, rearing, and finishing (Figure A7). Cattle are born and raised ("reared") on pasture, and most remain on pasture through the finishing (or fattening) stage, where they are brought to marketable weight before being transported to slaughterhouse plants for processing. Cattle production has long been concentrated in Brazil's Center-West region, with substantial expansion into the Amazon and Cerrado agricultural frontiers in recent decades. Because breeding, rearing, finishing, and processing do not necessarily occur in the same location, the industry forms a spatial supply chain in which cattle can move considerable distances before reaching processing plants.

An increasingly important alternative to a fully pasture-based system is confined finishing in feedlots. Feedlots do not generally replace pasture throughout an animal's life cycle: cattle are still born and reared on pasture but are moved into confinement for the final stage of production, where concentrated feeding allows them to reach slaughter weight more quickly. Historically, confined finishing played a relatively small role in Brazil compared with other major beef-producing countries. In 2001, approximately 6% of slaughtered cattle passed through feedlots; by 2024, estimates suggest that the share had risen to approximately 19% (ABIEC 2024). This expansion marks a shift toward a more capital- and input-intensive finishing technology. Confined finishing is particularly relevant for land use because faster weight gain and younger slaughter ages reduce the amount of time cattle spend grazing and therefore the pasture required to produce a given quantity of beef (de Vries, van Middelaar, and de Boer 2015).

The rapid expansion of feedlots coincided with the emergence of China as Brazil's dominant foreign beef market. Export access to mainland China is governed by bilateral sanitary requirements and granted at the plant level. The first plant-level authorizations occurred in the mid-2000s, but the economic importance of authorization rose sharply after the Chinese market reopened to Brazilian beef in 2015 and imports expanded rapidly. China has accounted for roughly half of Brazilian beef exports in recent years and is the foreign market with the largest exposure to deforestation associated with Brazilian beef supply chains (**?**). Importantly, beef destined for China is subject to production requirements that increase the value of rapid finishing, including a requirement that eligible cattle be slaughtered before 30 months of age (AQSIQ and MAPA 2015). Industry accounts explicitly link these requirements to the growth of confinement: exporters report premiums for younger, China-eligible cattle and describe feedlot or semi-intensive finishing as

an important means of meeting the age standard (Figueiredo 2022). While other developments in Brazil's cattle industry, such as the use of improved breeds, may explain part of the growth in observed output per hectare of pastureland in Brazil (Figure A8), in this paper I emphasize the role of feedlots in driving this productivity growth.[1]

Despite the growing importance of confined finishing in Brazil, systematic data on the location and development of feedlot capacity remain limited. Existing estimates of national feedlot activity are drawn largely from industry surveys, which provide useful aggregate measures of confined-cattle throughput but limited spatial and historical coverage of individual facilities. As a result, relatively little is known about where feedlot capacity has developed, when individual operations entered, or how this expansion relates spatially to processing plants and cattle-producing regions. I address this measurement gap by constructing a spatially explicit panel of Brazilian feedlots from high-resolution satellite imagery, allowing me to observe the location, physical footprint, and approximate entry date of confined-finishing operations over time.

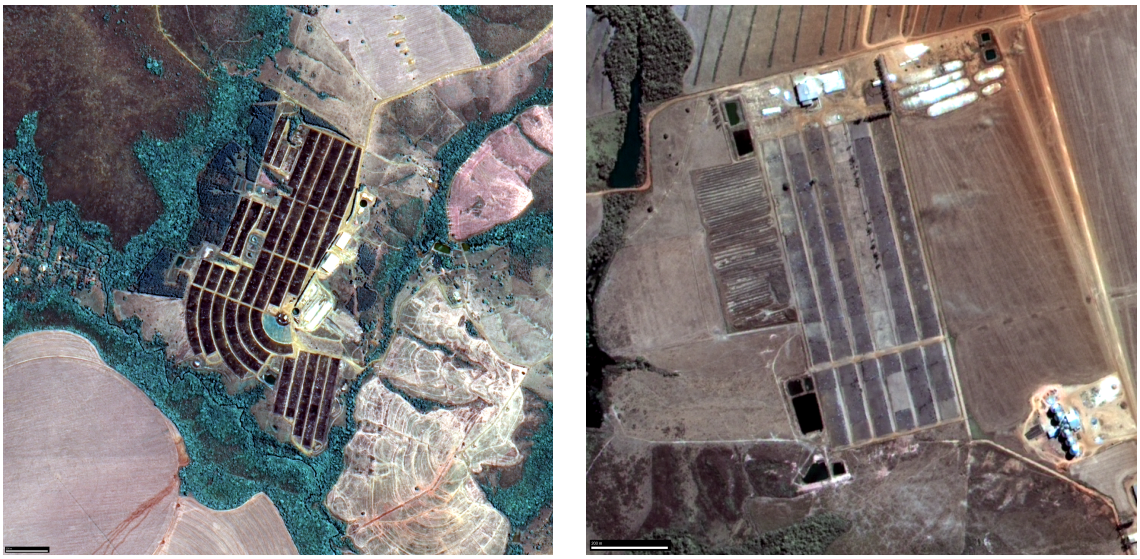
2.2 Measuring Feedlot Activity

Feedlot adoption is difficult to observe in existing data. To my knowledge, there is no public, facility-level record of Brazilian feedlots or of when they opened. I therefore construct one from satellite imagery in two steps: I first locate the feedlots operating in 2024 and then estimate the year each one opened. I define a feedlot as an open-air block of bare-earth pens where cattle are finished on feed, and I treat pens within 500 meters of each other as a single facility. To locate feedlots, I use freely available 2-meter color imagery from the CBERS-4A satellite, which covered 86% of Brazil's area in 2024. Pen layouts are plainly visible at this resolution (Figure 1 shows two such facilities). I train a convolutional neural network for object detection (YOLOv11) on image chips in which I outlined the pens by hand, along with chips that contain no feedlot. I start from the model that Aires, Martins, Hester et al. (2026) trained on U.S. feedlots and fine-tune it on Brazilian examples, which substantially reduces the number of labels required. The intuition behind this deep learning approach is simple: if I can recognize a feedlot by eye in the satellite imagery, the model can learn to see it too.

However, the model only proposes candidates. I inspected each candidate above a confidence threshold (determined by test sample performance) in both the 2-meter image and Google Earth, and kept it only if it showed an unambiguous pen structure.[2] I repeated

[1] Feedlots likely represent a bundle of productivity improvements. In addition to the main mechanism, the use of grain feed concentrates, these operations may also utilize feed additives to promote growth and have access to increased veterinary services, all of which can help to bring larger cattle to market more quickly.

[2] Most high-resolution images of feedlot sites contain clear imagery of cattle, which greatly aids in visually distinguishing feedlots from other agricultural scenes. This is due in large part to the distinct white color of the Nelore cattle, the most common breed in Brazil.



A. Goiás B. Mato Grosso

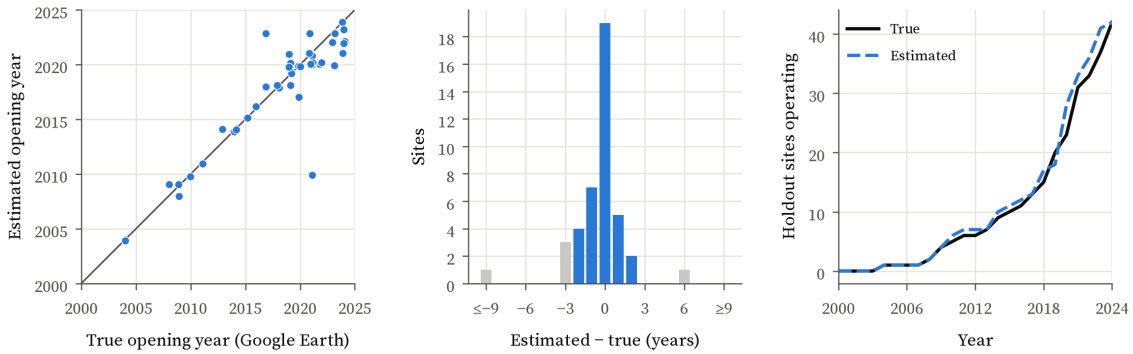
FIGURE 1. Two feedlots in 2-meter satellite imagery

Notes: Each panel shows a verified feedlot in the 2-meter CBERS-4A imagery used for detection. The pens are the dark, elongated blocks at the center of each image. The white bar in the lower-left corner of each panel marks 200 meters. The two panels are drawn at different scales.

this process over five rounds, adding confirmed feedlots and rejected look-alikes (e.g., crop fields, solar farms, and fish ponds) to the training data. Due to the manual verification process, the errors that remain are omissions rather than false inclusions.

A natural concern is that a model trained initially on feedlots that are predominantly located in the Center-West, where the industry is concentrated, simply finds more of what it already knows. I took three steps to guard against this. First, the model searched every available image in Brazil rather than pre-selected cattle regions. Second, I drew negative training examples from 15 land-cover classes nationwide and from the model's own false positives, balanced across states: the South supplies 3% of the positive examples but 29% of the negative ones. Third, I reviewed a similar share of candidates in every region (39–48%), even though far fewer turned out to be feedlots in the South (2%) than in the Center-West (8%). The regional pattern in the data (Table A1) is therefore designed to be representative of the underlying population of Brazilian feedlots and not merely a reflection of any targeted search effort.

To date each facility, I use the 30-meter Landsat archive from 1995 to 2026 (a median of 740 usable images per site). A feedlot pen is bare, compacted ground or concrete, so when a facility opens the site loses its vegetation and stops following the seasonal green-up of the surrounding land. I treat the opening as a structural break in the site's time series, measured relative to nearby land in the same image so that anything common to the image (e.g., haze or a drought year) cancels out. I combine two estimators: a multiple-break



A. Estimated versus true year B. Dating error C. Implied stock of feedlots

FIGURE 2. Validation of estimated opening years

Notes: The sample is the 42 holdout facilities whose opening I could date to an exact year in Google Earth's historical imagery. Panel A plots the estimated against the actual opening year, with the 45-degree line. Panel B shows the distribution of the estimated minus the true opening year. Panel C shows the number of holdout facilities operating in each year according to the true and the estimated opening years. Table A2 reports the corresponding accuracy measures.

regression (Bai and Perron 1998) on the pen footprint, in which both the level and the seasonal cycle can shift, and a single-break regression estimated pixel by pixel, with pixels voting on the year. When these estimators err, they tend to err early because they pick up earlier land clearing at the site, so I take the later of the two dates.

I evaluate both steps against hand-labeled data. In municipalities that contributed no training examples, the detector finds roughly 90% of 111 labeled facilities. For opening years, I dated a stratified sample of 308 facilities by hand using Google Earth's historical imagery, setting aside 100 as a holdout before labeling and scoring them only once the estimation process was fine-tuned using the labeled development set. Among the 42 holdout facilities whose opening can be pinned to an exact year, 74% of estimates fall within one year and 88% within two, with a median error of zero (Figure 2). The estimates correctly classify whether a facility is operating in 95% of site-years, which is the relevant margin for my panel analysis.

The dataset provides a lower bound on the total feedlot capacity in 2024 rather than the complete population of facilities. Every facility in my dataset is manually verified, but the detector likely misses some feedlots, particularly small ones, and areas not imaged in 2024 were never searched. The resulting dataset contains 1,693 verified facilities in 778 municipalities and 24 of Brazil's 27 states, which I aggregate to counts of operating feedlots by municipality and year. Appendix A provides further detail on the input data and detection methodology.

2.3 Other Data Sources

I combine the feedlot panel with data on beef plants and their access to the Chinese market, cattle herds and movements, and land use.

China market access. Brazilian slaughterhouses are inspected at the federal, state, or municipal level, and only plants under the Federal Inspection Service (Serviço de Inspeção Federal, SIF) may export. I take the location, owner, inspection level, and capacity of 1,304 beef plants, 224 of them federally inspected, from the facility dataset that Trase (2025) compiles from public inspection registries. By 2024, China had authorized 67 of the federally inspected plants, 52 of them in 2019 or later. I obtained the date of each authorization from the Ministry of Agriculture through requests under Brazil's access-to-information law (Lei de Acesso à Informação, LAI). These records, together with plant lists reported in the trade press, also show when each plant was first nominated to the Chinese authorities, including plants that were nominated but not approved. I measure Chinese import demand and Brazilian beef exports to China with the BACI bilateral trade data. To measure access to plants, I compute the shortest distance over the OpenStreetMap road network from each of 7.9 million rural properties to every plant and average across the properties in a municipality, weighting by area.[3] Property boundaries come from the Rural Environmental Registry (Cadastro Ambiental Rural, CAR), in which landholders must register their properties.

Beef industry data. An animal transit permit (Guia de Trânsito Animal, GTA) must be issued whenever cattle are moved between properties or to slaughter. State animal health agencies hold these records, and I use the ones published by Mato Grosso, the state with the largest herd, for 2013 onward, and by Pará and Espírito Santo for recent years. Each record reports the origin and destination municipality, the date, the purpose of the movement (e.g., rearing, finishing, or slaughter), and the number, sex, and age class of the animals. The Mato Grosso files alone contain 13.8 million records. I use the permits to measure the age of cattle sent to slaughter and to trace where plants and feedlots source their animals. In addition, I take the cattle herd of each municipality in each year from the Municipal Livestock Survey (Pesquisa da Pecuária Municipal, PPM) of the Brazilian Institute of Geography and Statistics (IBGE). For validation of estimates derived from these aggregated transit records, I use freight orders from JBS, Brazil's largest meatpacker, published by Dias, Vieira e Silva, Maciel e Silva et al. (2025). They cover deliveries to 38 plants from 2018 to 2020 and record the receiving plant, the road distance, and the average

[3] I observe the road network in 2026, and the road network in 2026 may vary from the network in the beginning of my sample. Unfortunately, comprehensive and historical road data is not easily accessible for Brazil, so I opt to use a recent source to ensure the best possible coverage in remote regions.

age and carcass weight of each shipment. However, the shipment origins are anonymized, limiting the use of these data beyond validation.

Land use. I measure land use with the annual land-cover maps of MapBiomas Project (2025), which classify every 30-meter pixel in Brazil from Landsat imagery in each year since 1985. From these maps, I compute pasture area by municipality and year and the area converted to pasture from each other land-cover class, such as forest and savanna. To translate this conversion into potential carbon losses, I use the carbon stock per hectare of each land-cover class in each biome from Brazil's Fourth National Greenhouse Gas Inventory, as matched to the MapBiomas classes by SEEG (2024).

3 Descriptive Evidence

Observation 1: Most of Brazil's feedlot capacity was built during the China export boom. The first three Brazilian plants were authorized to export directly to mainland China in 2005, but Chinese import demand did not ramp up until 2015 (Figure 3). Feedlot construction is concentrated in the same years. Of the 1,693 feedlots I detect in 2024, 74% opened in 2015 or later, and these facilities hold 66% of total pen area. The top panel of Figure 3 plots the finishing margin, which I define as the market value of a finished steer minus the price of a feeder calf, in real prices. It measures the gross return to bringing a calf to slaughter weight, before feed and other costs. The margin moved between roughly R$1,900 and R$2,300 per head from 2008 to 2018, then rose 86% between 2018 and 2022 as exports to China nearly quadrupled. In 2023 it was still 38% above its 2018 level. Recent feedlot entry is therefore concentrated in the years when exports were booming and the economic incentive to finish cattle was high.

Observation 2: Feedlot capacity is concentrated where access to China-authorized plants is high, and this exposure varies greatly across cattle-producing regions. I measure a location's physical access to China-authorized plants as the sum of the inverse road distances to the 67 plants authorized by 2024, so access is highest where several authorized plants are nearby. Figure 4A maps this measure together with the feedlots, which cluster in the high-exposure regions. Access differs widely across the places that raise cattle. Weighting municipalities by the size of their herd, China-authorized plant exposure at the 90th percentile in 2024 is 3.3 times exposure at the 10th percentile, compared with a ratio of 2.9 for access to all other slaughter plants. The clustering of feedlots does not simply mirror the distribution of cattle. Figure 4B ranks municipalities from highest to lowest access and plots the cumulative share of feedlot pen area against the cumulative share of the cattle herd. If feedlots were located in proportion to cattle, the curve would lie on the 45-degree line. Instead, the best-access municipalities that together hold 30% of

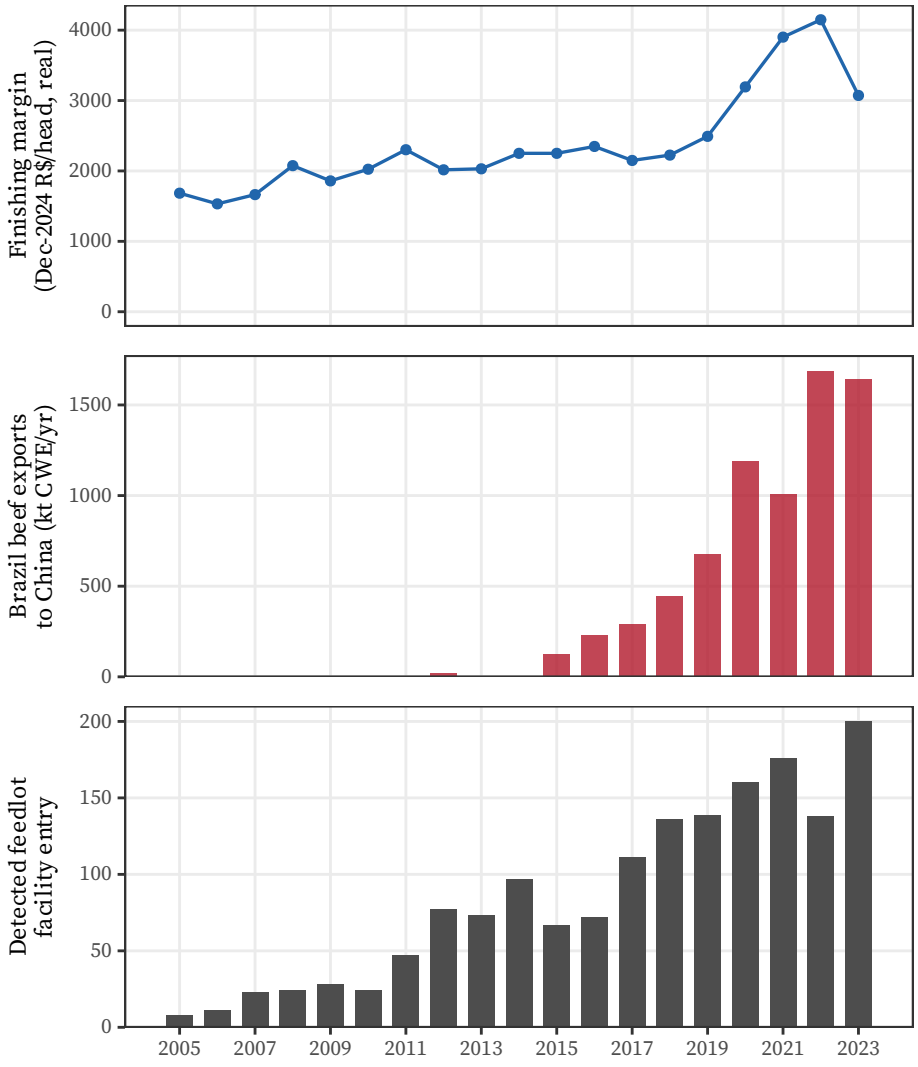


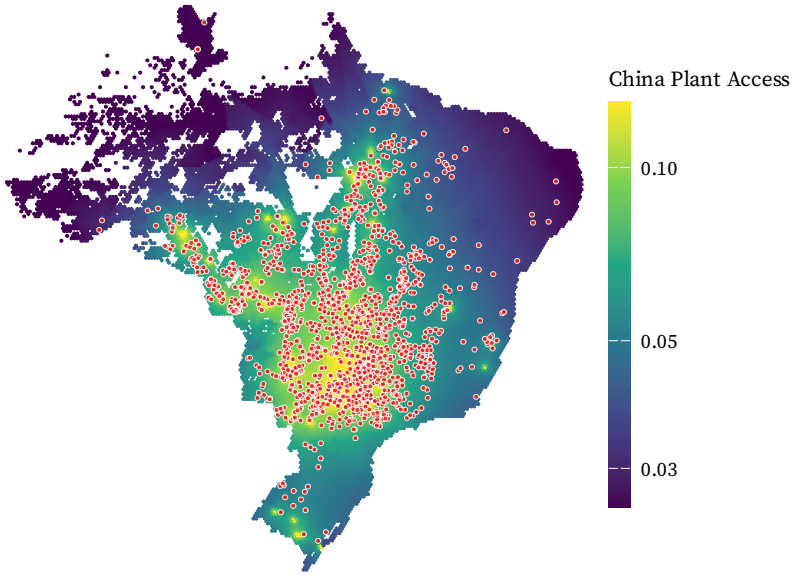
FIGURE 3. Finishing margin, beef exports to China, and feedlot openings, 2005 to 2023

Notes: The top panel shows the annual average finishing margin: the value of a finished steer (the São Paulo price of finished cattle times the national average carcass weight of steers) minus the price of a feeder calf in Mato Grosso do Sul, deflated by the consumer price index (IPCA) to December 2024 reais per head. Feed and other finishing costs are not deducted. The middle panel shows Brazilian beef exports to mainland China in thousand tonnes of carcass-weight equivalent (CWE). The bottom panel shows the feedlots detected in 2024 by estimated opening year. Prices are from CEPEA, carcass weights from IBGE, and trade flows from BACI.

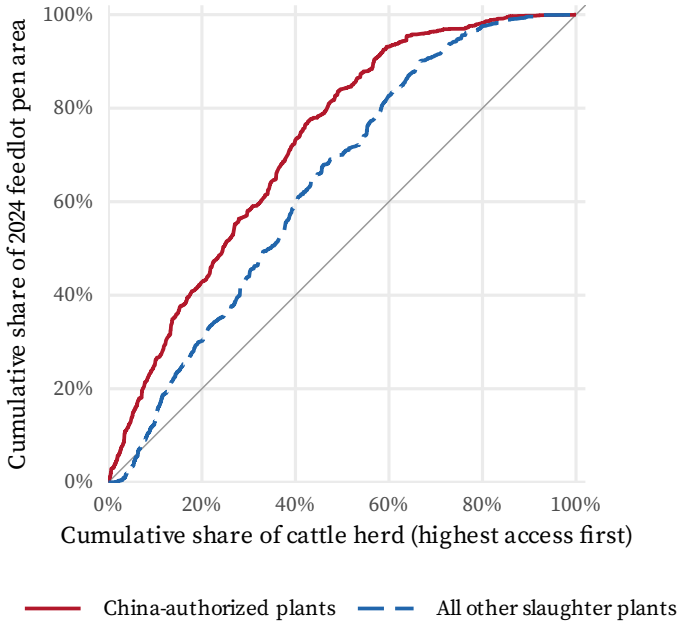
the herd contain 58% of pen area. When I rank municipalities by their access to all other slaughter plants, the same share of the herd contains 44% of pen area, so feedlots are tied to China-authorized plants in particular and not only to slaughter capacity in general. These patterns show that feedlots and China-authorized plants locate together, but they cannot show which came first. They could reflect the siting of authorization, if approval went to plants in regions where feedlot finishing was already established, or the sorting of feedlots toward plants that gained access to China.

Observation 3: Municipalities with China-authorized processing plants increasingly source from feedlot municipalities, and source younger cattle. Animal transit permits (GTA) from Mato Grosso, the state with Brazil's largest cattle herd, record the origin, destination, month, and age class of cattle shipments originating in the state since 2013. I use them to compare slaughter in the seven municipalities whose plants were first authorized in 2019 with slaughter in municipalities that have no authorized plant. Figure 5A shows the share of slaughter cattle that arrive from a municipality with a feedlot, with a clear divergence forming in 2019 as China-authorized municipalities increasingly source from feedlot regions. The cattle are also younger. From 2013 to 2018, cattle aged 24 months or less made up 13% of slaughter in authorized municipalities and 12% in never-authorized ones. In 2024 they made up 43% and 28%, respectively. Of this 15 percentage point gap, 6 points arise because authorized municipalities buy from a different set of origin municipalities and 9 points because they receive younger cattle from the same origins. Figure 5B shows how the change is spread both within years and over time. The share of young cattle sourced peaks between August and November, when feedlot finishing is highest in Mato Grosso, and the share of cattle older than 36 months peaks in the first months of the year, when pasture finishing is concentrated. Plants appear to respond to China authorization by sourcing younger cattle from regions with feedlots. Slaughter age is a direct indicator of productivity growth and it matters for land use: an animal slaughtered younger spends less time on pasture, so less grazing land is needed to produce a given amount of beef each year.

Observation 4: Plants and feedlots draw cattle over long distances. Figure 6 shows the cumulative distribution of the distance cattle travel to slaughter. In freight orders covering 19 million cattle delivered to 38 plants of JBS, Brazil's largest meatpacker, from 2018 to 2020 (Dias, Vieira e Silva, Maciel e Silva et al. 2025), the median animal travels 173 km by road, 42% travel more than 200 km, and 21% travel more than 300 km. Transit permits give a similar distribution for Mato Grosso, with a median of 156 km, and somewhat shorter hauls in Espírito Santo and Pará, although the latter state's distribution exhibits a long tail due to its location on the agricultural frontier. Feedlots source more of their cattle locally, but their reach is also wide (Figure A9). The grazing land serving a feedlot or a processing plant is therefore not necessarily near where it operates, which is why I trace



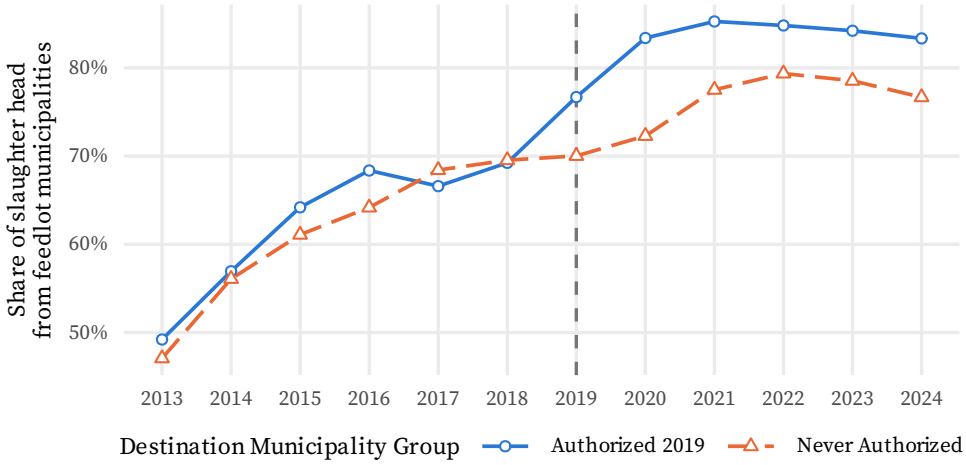
A. Access to China-authorized plants and feedlot locations



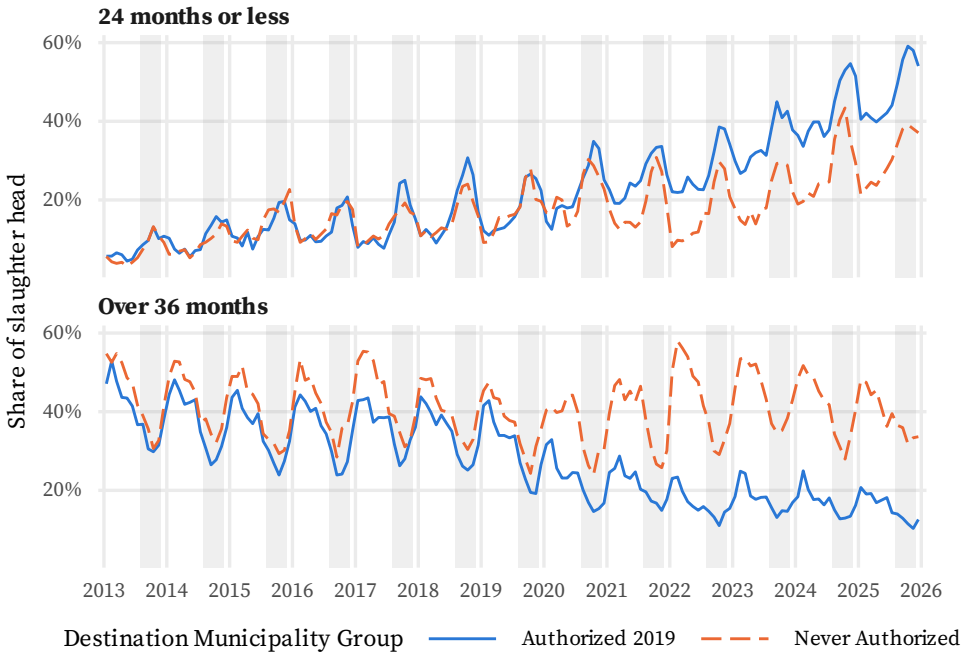
B. Feedlot pen area and the cattle herd, by plant access

FIGURE 4. Feedlots and access to China-authorized plants

Notes: Access to China-authorized plants is the sum, over the 67 plants authorized by 2024, of the inverse road distance from a rural property to each plant. Access is shown on a logarithmic scale. Cells with no registered rural property are blank. Red dots mark the feedlots detected in 2024. Panel B averages access across the properties in each municipality, weighting by property area, ranks municipalities from highest to lowest access, and plots the cumulative share of 2024 feedlot pen area against the cumulative share of the 2024 cattle herd. The solid line ranks municipalities by access to China-authorized plants and the dashed line by access to all other slaughter plants, measured in the same way.



A. Share of slaughter cattle from municipalities with feedlots



B. Monthly share of slaughter cattle by age

FIGURE 5. Slaughter cattle in Mato Grosso by China authorization status

Notes: Based on animal transit permits for cattle shipped to slaughter within Mato Grosso. "Authorized 2019" groups the seven municipalities whose first China-authorized plant was approved in 2019. "Never Authorized" groups the municipalities that receive slaughter cattle and have no authorized plant. Panel A shows the share of slaughter cattle that come from a municipality with detected feedlot pen area in that year. The dashed vertical line marks 2019. Panel B shows the monthly sourcing shares of slaughter cattle aged 24 months or less and over 36 months. Shaded bands mark August to November, when feedlot production cycles are concentrated in Mato Grosso.

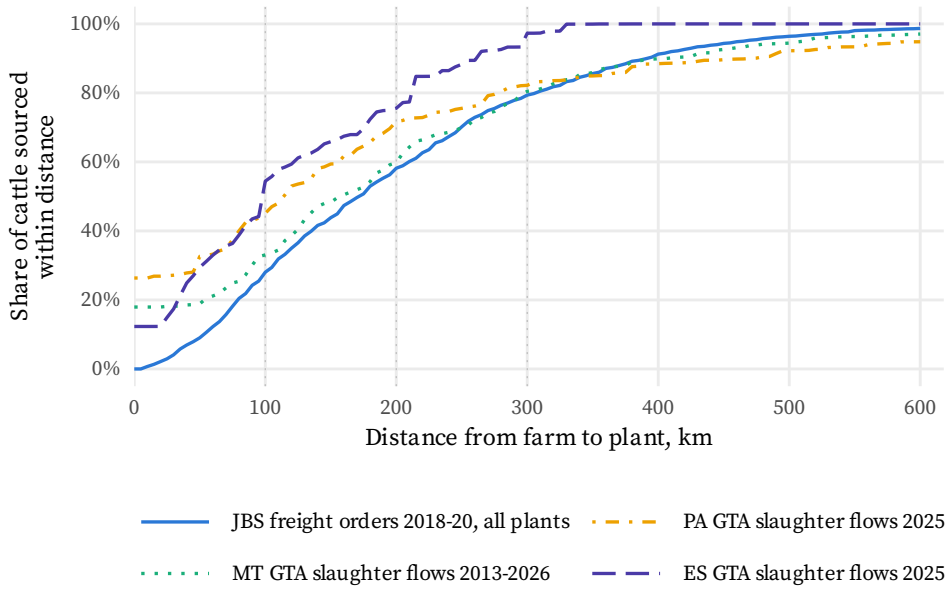


FIGURE 6. Distances cattle travel to slaughter plants

Notes: The figure shows the cumulative share of cattle delivered to slaughter by distance traveled. The JBS series uses shipment data from Dias, Vieira e Silva, Maciel e Silva et al. (2025), which reports exact road distances. The other series use animal transit permits (GTA) for Mato Grosso (MT), Pará (PA), and Espírito Santo (ES). For the GTA series, distance is measured between municipality centroids, and movements within a municipality are assigned a distance of zero.

land requirements upstream through the cattle sourcing network in Section 5.

4 Empirical Approach

The goal of this section is to estimate the effect of exposure to the Chinese export market on feedlot entry. In the ideal experiment, export authorization would be assigned at random to plants across regions, and I would compare feedlot entry in the regions around authorized plants with entry around plants that were not authorized. This is the benchmark that I try to approximate: variation in access to the Chinese market across locations that is unrelated to other determinants of feedlot growth.

My setting departs from this benchmark in two main ways. First, access to China may arrive alongside other changes. Regions that gained access earlier may also have received road improvements, new processing capacity, credit, or technical assistance, which makes it difficult to separate the effect of export demand from the effect of everything that came with it. Second, causality could run in the other direction. Regions that had already developed finishing capacity and processing infrastructure may have been more attractive candidates for authorization. A related concern is selection on anticipated growth: the

plants that Brazil nominates may be those expected to expand, or those whose owners committed to new investment in order to serve Chinese demand.

The event study addresses these concerns only in part. To limit the role of unobserved regional differences, I compare only municipalities near plants that are eventually authorized, so that the estimates come from when a municipality gains access and not from selection into the authorization pool. To assess reverse causality, I examine whether feedlot entry evolved similarly in earlier- and later-exposed municipalities before exposure. Neither step entirely rules out selection on anticipated growth, which are not guaranteed to appear in pre-exposure trends. However, I subsequently build on the logic of the event study design to to better address each of these concerns.

4.1 Event Study

Access to China is determined in three steps. The two governments first agree on country-level sanitary requirements. Brazil's Ministry of Agriculture (MAPA) then evaluates Brazilian plants and recommends batches of candidates, and the Chinese authorities audit the recommended plants and make the final registration decision (General Administration of Customs of the People's Republic of China 2021). Each step likely reflects diplomatic negotiations, lobbying by large processors, demand conditions in China, and shocks to competing exporters. However, the final step is outside the control of Brazilian producers and difficult for them to predict. For example, China authorized no Brazilian beef plant between November 2019 and March 2023, although plants nominated in 2019 were still awaiting a decision. Plants on the same list were therefore authorized several years apart.

I first estimate the effect of accelerated China access with the staggered difference-in-differences estimator of Callaway and Sant'Anna (2021). Let Y_{it} denote the cumulative number of feedlots opened in municipality i through year t, per 100,000 head of the municipality's average herd over 2000 to 2004, and let G_i denote the year in which i is first exposed.[4] For the municipalities first exposed in year g, the effect of exposure in year $t \geq g$ is

$$ATT(g,t) = \mathbb{E}\left[Y_{it} - Y_{i,g-1} \mid G_i = g\right] - \mathbb{E}\left[Y_{it} - Y_{i,g-1} \mid G_i > t\right]. \tag{1}$$

Intuitively, this estimator takes the growth in feedlots since the year before exposure in the newly exposed municipalities and subtracts the growth over the same years in municipalities that are not yet exposed. I then average these comparisons across cohorts by the number of years since exposure, weighting each cohort by its number of municipalities. I report estimates from six years before to twelve years after exposure, because longer horizons are identified from the 2005 cohort alone.

[4] I observe the feedlots that operate in 2024, so the count for an earlier year omits any facility that opened and closed before then.

These estimates can be interpreted as an average treatment effect on the treated (ATT) under two assumptions. The first is parallel trends. That is, absent exposure, feedlot entry in the municipalities exposed in year g would have followed the same path as in the municipalities exposed later. The second is no anticipation: feedlots do not open in response to an authorization before it occurs. The estimates for the periods before exposure provide a check on both.

4.2 Sample Overview

China authorized the 67 plants in seven years between 2005 and 2024, which I refer to as authorization waves (Figure 7). I use these waves to define when each municipality first gained access to the Chinese market. Specifically, I consider a municipality exposed once at least half of its rural property area lies within 200 km by road of an authorized plant, and I assign it to the wave in which this first occurs. The choice of 200km is partly arbitrary and represents an attempt to isolate a local effect. [5] I also estimate the event study at different sourcing radii.

Table 1 summarizes the resulting cohorts. My main sample is the 1,628 municipalities that are exposed to an authorized plant by 2024, which I observe annually from 2003, the earliest opening year in the feedlot data, to 2023. On average over 2000 to 2004, these municipalities held 107 million head of cattle, or 57% of the national herd, and they contain 1,120 of the 1,631 feedlots that had opened by 2023. The largest cohort is the 485 municipalities first exposed in 2019, when China authorized 22 plants, and feedlots were rare everywhere at the start of the sample.

Because the panel ends in 2023, the municipalities first exposed in 2024 are never exposed within the sample and serve only as controls. The remaining 3,902 municipalities are never within 200 km of an authorized plant. I exclude them from the main sample because regions far from any authorized plant likely differ from exposed regions in ways that also affect feedlot growth, and I use them only in an alternative specification. In the main specification, every comparison is therefore between municipalities that eventually gain access to an authorized plant and differ in when they gain it.

4.3 Results

Figure 8A presents the main estimates. Before exposure, feedlot entry evolves similarly in earlier- and later-exposed municipalities and no lead is statistically distinguishable from zero. After exposure, feedlot entry rises steadily. The estimate reaches 0.20 after four years and 0.54 after twelve, which is 42% of the average level across sample municipalities

[5] For context, 58% of the cattle delivered to JBS plants travel 200 km or less (Figure 6).

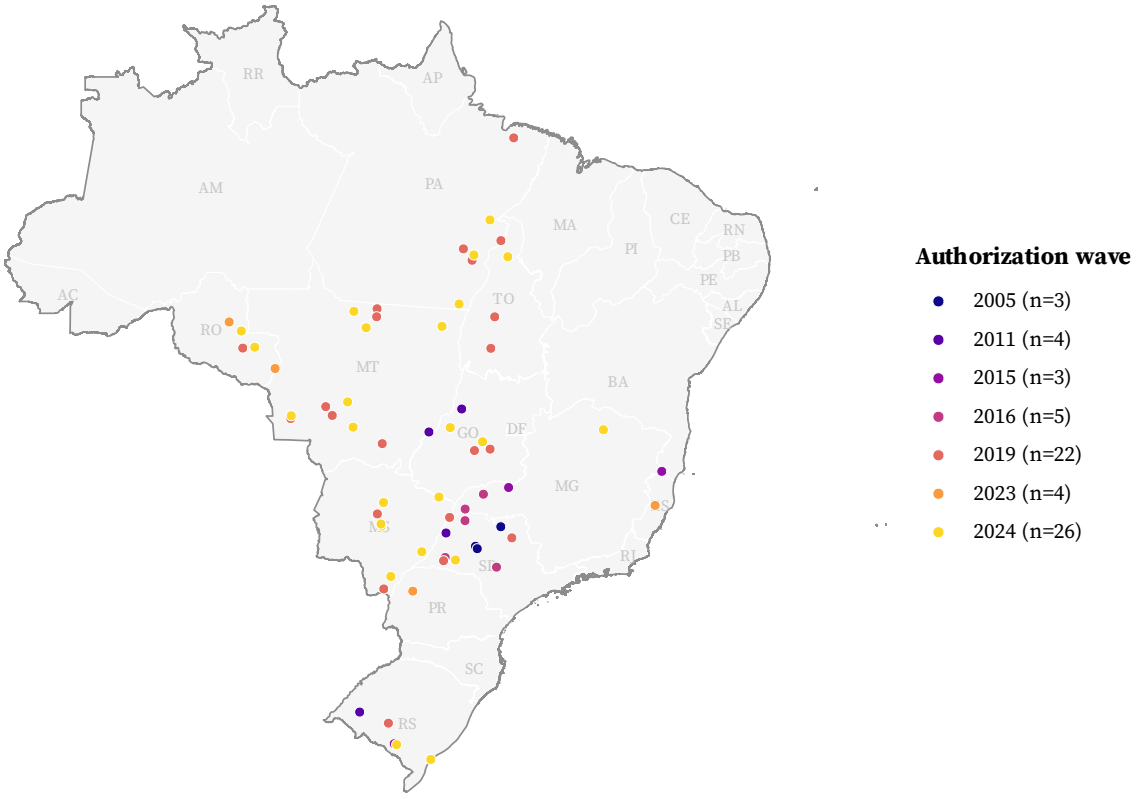


FIGURE 7. Beef plants authorized to export to China, by authorization wave

Notes: Each dot is one of the 67 beef plants authorized to export to mainland China by 2024, colored by its authorization wave, with the number of plants in each wave in parentheses. Gray labels are state abbreviations.

in 2023. Averaged over years 0 to 12, exposure raises the number of feedlots by 0.27 per 100,000 head.

Figure 8B repeats the estimation with the 3,902 never-exposed municipalities as the comparison group. The post-exposure estimates are larger, but so are the differences before exposure. Exposed municipalities therefore appear to have been adding feedlots faster than never-exposed municipalities before any nearby plant was authorized. This is the pattern I would expect if regions far from authorized plants are on a different trajectory, which motivates the use of the later-treated comparison group. The results are similar with an alternative estimator. The interaction-weighted estimator of Sun and Abraham (2021) gives an average effect of 0.20 over the same years, and Figure A4 in Appendix B shows the full path.

If these estimates reflect access to authorized plants, the response should be stronger closer to the plant, where producers are most likely to supply it. To test this, I date exposure by the first year in which a municipality is within 300 km of an authorized plant and group municipalities by their distance to the plant at that date: within 100 km, between 100 and

TABLE 1. Authorization waves and the event-study sample

Authorization wave	Plants	Municipalities	Herd (million head)	Feedlots open by 2004	Feedlots open by 2023	Feedlots per 100,000 head
2005	3	351	10.0	4	220	2.37
2011	4	141	15.6	2	129	0.79
2015	3	138	9.3	0	59	0.71
2016	5	200	9.0	3	108	1.50
2019	22	485	42.1	5	457	1.24
2023	4	164	6.2	0	26	0.17
2024	26	149	15.0	0	121	0.75
All exposed by 2024	67	1,628	107.3	14	1,120	1.28
Never exposed		3,902	79.4	6	499	0.33

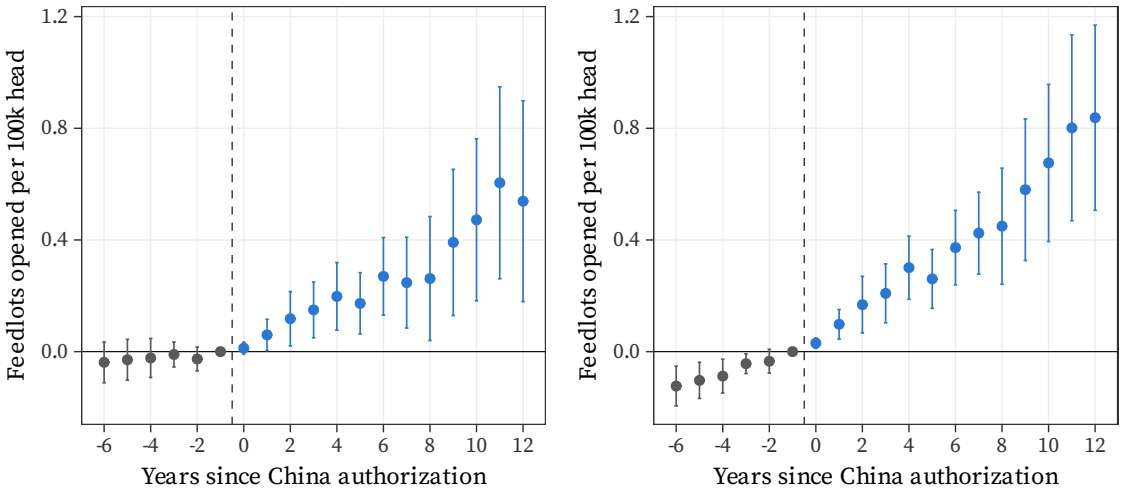
Notes: A municipality is exposed in the first year in which at least half of its rural property area lies within 200 km by road of a plant authorized to export to China. Plants is the number of plants authorized in each wave, and Municipalities is the number of municipalities first exposed in that wave. The 2024 wave is not exposed within the 2003 to 2023 panel and serves only as a comparison group. Herd is the average municipal cattle herd over 2000 to 2004. Feedlots are the count of detected facilities that had opened by the end of the given year. The last column is the average across municipalities of the feedlots open by 2023 per 100,000 head of the 2000 to 2004 herd.

200 km, or between 200 and 300 km. I then estimate the event study separately within each group, so that the comparison is always with municipalities at the same distance that are exposed later. Figure 9 shows a clear gradient. The average effect over years 0 to 12 is 0.48 feedlots per 100,000 head within 100 km, 0.23 between 100 and 200 km, and 0.12 between 200 and 300 km. This gradient is difficult to explain with regional shocks that happen to coincide with authorizations, which I would not expect to weaken monotonically with distance to the authorized plant.

4.4 Timing Placebo

The event study treats the timing of authorization as unrelated to local trends in feedlot entry. As a check, I ask how unusual the estimated path is relative to the paths I obtain when authorization dates are assigned at random. I hold fixed the 67 plants and the number of plants authorized in each wave, randomly reassign the authorization years across plants, recompute each municipality's year of first exposure, and re-estimate the event study. I repeat this procedure 1,000 times. Because every plant is still authorized in some wave, the set of exposed municipalities does not change. Only the timing of their exposure does.

Figure A5A in Appendix B plots the placebo paths together with the actual estimates. The actual path lies above the median placebo path in every year after the initial year of exposure, while only 22 of the 1,000 placebo paths achieve this. Figure A5B summarizes each path by its average effect over all years after exposure, including horizons beyond twelve years. The actual average is 0.61, compared with a placebo median of 0.08, and only



A. Not-yet-exposed controls

B. Never-exposed controls

FIGURE 8. Feedlot entry before and after exposure to a China-authorized plant

Notes: Each panel shows event-study estimates relative to the year before authorization exposure. The outcome is the cumulative number of feedlots opened per 100,000 head of the municipality's 2000 to 2004 average herd. In Panel A, the sample is the 1,628 municipalities exposed by 2024 and the comparison group is the municipalities not yet exposed. In Panel B, the comparison group is all municipalities that are never exposed. Bars are pointwise 95% confidence intervals from a multiplier bootstrap clustered by geographic region, defined by the IBGE.

2.8% of the placebo draws are as large in absolute value.

The placebo paths are not centered on zero, however. The median placebo path drifts upward after exposure and reaches about 0.1 feedlots per 100,000 head. This drift arises because plants are not spread evenly across space. Municipalities surrounded by many plants are reached early under almost any assignment of dates, and they are also the cattle regions where feedlots grew fastest. In other words, municipalities differ in the exposure they can expect, even when the timing of authorization is random. A comparison of earlier- and later-exposed municipalities therefore reflects part of this difference. In addition, a random reshuffling of dates across all 67 plants is only a coarse approximation of how authorizations were assigned in practice. I address both issues in the next section.

4.5 Recentered Exposure Design

In this section, I separate the part of a municipality's exposure that follows from its location-specific and endogenous characteristics from the exposure that arises due to the idiosyncratic nature of the authorization process. I do so with the recentering approach of Borusyak and Hull (2023), henceforth BH.

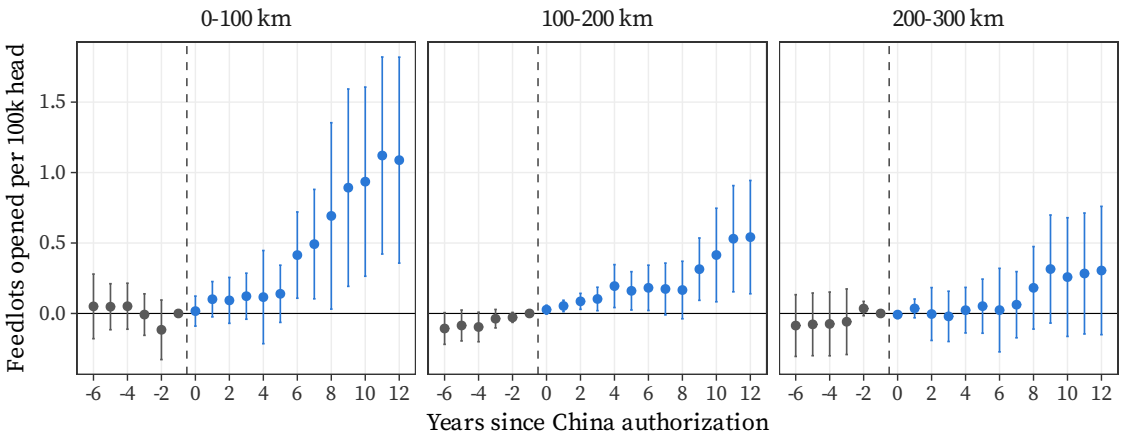


FIGURE 9. Feedlot entry after exposure, by distance to the authorized plant

Notes: Each panel shows event-study estimates relative to the year before authorization exposure. Municipalities are grouped by whether, at that date, the same share of their area is also within 100 km, within 200 km, or only within 300 km. Each panel is estimated separately, and the comparison group is the municipalities in the same distance group that are not yet exposed. The panels include 297, 765, and 1,231 municipalities. Bars are pointwise 95% confidence intervals from a multiplier bootstrap clustered by immediate geographic region, defined by the IBGE.

Approach. The event study treats access to the Chinese market as a binary event, dated by the first authorization of a plant within 200 km. However, the value of an authorization changed sharply over the sample period. China's beef imports from countries other than Brazil rose from 0.04 million tonnes in 2011 to 1.9 in 2022, so a plant authorized in 2011 gave its suppliers access to a far smaller market than a plant authorized in 2019. I therefore weight access by Chinese import demand and refer to this measure as China export *exposure*. Let a_p denote the year in which China authorizes plant p, and let D_t denote China's beef imports from all countries other than Brazil in year t, in million tonnes of carcass weight. The exposure of municipality i in year t is

$$X_{it} = D_t \sum_p w_{ip} \mathbf{1}\{a_p \leq t\}, \tag{2}$$

where $w_{ip} \in (0, 1)$ measures the physical access of municipality i to plant p. I compute w_{ip} as the area-weighted average, over the rural properties in i, of a weight that declines nonlinearly with the road distance from the property to the plant.[6] I use imports from other countries so that D_t reflects Chinese demand for foreign beef and not the supply response of Brazilian producers. This demand grew because Chinese consumption outpaced domestic production: imports supplied about 6% of the beef consumed in mainland China in 2014 and about one third in 2024 (USDA Foreign Agricultural Service 2026).

[6] I choose this rate of decay to match the distribution of farm-to-plant shipping distances reported by Dias, Vieira e Silva, Maciel e Silva et al. (2025).

My measure of treatment is cumulative exposure from 2005 to 2024,

$$C_i = \sum_{t=2005}^{2024} X_{it} = \sum_p w_{ip}\, c(a_p), \qquad c(a) = \sum_{t=a}^{2024} D_t, \tag{3}$$

measured in million tonne-years (Mt-years). The second expression shows that exposure is a weighted sum of shocks to import demand that plants in i's network face. The shock $c(a_p)$ is a measure of the Chinese demand that plant p could serve after its authorization: 10.5 Mt-years for a plant authorized in 2019, 1.7 for a plant authorized in 2024, and zero for a plant that was never authorized. The outcome is the change in the municipality's stock of feedlots over the same period, $\Delta Y_i = Y_{i,2024} - Y_{i,2004}$, where Y_{it} is either the number of feedlots or their total pen area.[7] Because no plant was authorized before 2005, exposure is zero everywhere in 2004, so both variables are changes from a common starting point. The long difference also allows me to use pen area, which measures capacity directly: I observe the pen area of each facility in 2024, and with a single difference I do not need to date its expansion year by year, which is difficult to estimate at the resolution of the available historical imagery for Brazil. Pen area is a particularly useful outcome measure in this context as it directly maps to the total potential finishing capacity, conditional on the number of cycles or "turns" operated per year in a facility.

A regression of ΔY_i on C_i compares municipalities with high and low exposure, and exposure can be high for two different reasons. A municipality may be surrounded by many plants that are candidates for authorization, or the plants around it may have been authorized early. The first source of variation reflects where the beef industry was already concentrated, which is the selection on location that the event study results do not rule out. Recentering isolates the second source. The idea is to treat the vector of authorization years as the outcome of an assignment process and to specify the alternative assignments that this process was equally likely to produce. Each alternative implies a full path of exposure for every municipality through equations (2) and (3). Averaging over the alternatives gives expected exposure, μ_i, which is the exposure that municipality i would receive on average given only its position relative to the candidate plants. Recentered exposure is the difference between the two,

$$\tilde{C}_i = C_i - \mu_i. \tag{4}$$

Intuitively, μ_i is what location predicts and $\tilde{C}_i$ captures the luck of the draw: whether the plants near i were authorized earlier or later than a typical candidate. By construction, $\tilde{C}_i$ has mean zero for every municipality, whatever its location, so in expectation it is

[7] My working assumption, absent additional evidence, is that the rate of feedlot entry over my period of study dominates the rate of any facility exit, which supports the interpretation of ΔY_i as a measure of capacity growth. If there was a non-trivial level of exit, then my estimates measure the effect on persistent new capacity. If survival itself responds to exposure, the estimate combines the two margins.

uncorrelated with any fixed characteristic of the municipality, observed or not. This property does not require plants to be located at random. It requires that I specify the assignment process correctly, that is, which plants could have been authorized in place of the ones that were.

The timing placebo assumed that any of the 67 authorized plants could have received any authorization date. This assumption is too strong, because Brazil nominates groups of plants for approval at different times and China could only choose among the plants that had been nominated. I use the nomination record, determined to the best of my ability, to group candidate plants into two queues. The first contains the 15 plants that Brazil nominated in the mid-2000s. A 2010 circular of the Ministry of Agriculture obtained via a LAI request documents this group as the plants that Brazil had nominated, and Chinese inspectors had visited, before negotiations resumed in that year (Ministério da Agricultura, Pecuária e Abastecimento 2010). China authorized three of them in 2005, four in 2011, three in 2015, and five in 2016. The second queue contains 58 plants that were candidates from 2019 onward: the 52 plants authorized in 2019, 2023, and 2024, and six plants that Brazil nominated but China had not authorized by 2024.

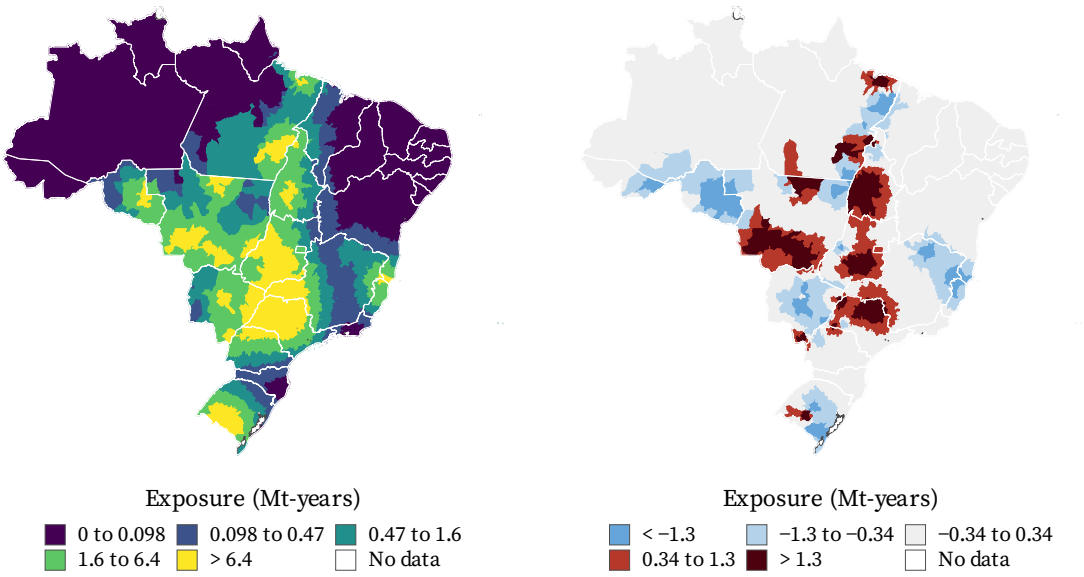
My identifying assumption is that, within a queue, the order in which China authorized plants is unrelated to other determinants of feedlot growth in the surrounding municipalities. Brazil's decision to nominate a plant may well reflect the plant's prospects, and the queues condition on that decision. The variation that remains is China's choice of which nominated plants to approve and when, which depended on its own audits and on long pauses in approvals that Brazilian producers did not control (Section 4.1).

Under this assumption, any reassignment of the realized authorization years among the plants of a queue was as likely as the one that occurred. I therefore construct the alternative assignments by permuting authorization years within each queue, which holds fixed the number of plants authorized in each wave. Expected exposure is then $\mu_i = \sum_p w_{ip}\,\bar{c}_{q(p)}$, where $\bar{c}_{q(p)}$ is the average shock among the plants in the queue of plant p, and recentered exposure becomes

$$\tilde{C}_i = \sum_p w_{ip}\left[c(a_p) - \bar{c}_{q(p)}\right]. \tag{5}$$

Recentered exposure is positive where nearby plants were authorized earlier than the average plant in their queue and negative where they waited. In the second queue, a plant authorized in 2019 received 5.5 Mt-years more than the queue average, and a plant still unauthorized in 2024 received 5.0 Mt-years less. Appendix C lists each step of the construction.

Figure 10 maps the two measures. Realized exposure (Panel A) is concentrated in a band from São Paulo through Goiás and Mato Grosso, where plants are dense, and it is



A. Realized exposure, C_i

B. Recentered exposure, $\tilde{C}_i$

FIGURE 10. Realized and recentered exposure to Chinese beef demand, 2005 to 2024

Notes: Panel A shows each municipality's cumulative exposure to Chinese beef import demand through authorized plants from 2005 to 2024, in million tonne-years (Mt-years). Panel B shows recentered exposure, which is realized exposure minus the exposure expected when authorization years are permuted among the plants in the same nomination queue. White lines are state borders.

close to zero in the North and Northeast. Expected exposure is nearly the same map: it accounts for 98% of the variance of realized exposure across municipalities. Recentered exposure (Panel B) looks different. It is close to zero in most of the country, and within the main cattle regions it takes both signs. For example, municipalities in western Mato Grosso, Goiás, and Tocantins received more exposure than expected, while municipalities in Rondônia and Mato Grosso do Sul received less.

I use recentered exposure in three specifications. The first two apply BH directly. The recentered IV estimates

$$\Delta Y_i = \alpha + \beta\, C_i + X_i'\delta + \varepsilon_i \tag{6}$$

by two-stage least squares, with $\tilde{C}_i$ as the instrument for C_i. The second specification adds expected exposure as a control and is estimated by OLS,

$$\Delta Y_i = \alpha + \beta\, C_i + \gamma\, \mu_i + X_i'\delta + \varepsilon_i. \tag{7}$$

Because $C_i = \mu_i + \tilde{C}_i$, holding μ_i fixed leaves only recentered exposure to identify β, so the comparison is among municipalities with the same expected exposure. The coefficient γ

has no causal interpretation: it measures how feedlot growth varies with the geography of candidate plants. BH recommend this form over the IV in natural experiments, in which the assignment process is assumed and not known. In both linear specifications, I measure ΔY_i per 100,000 head of the municipality's 2000 to 2004 cattle herd, the unit of the event study, and weight municipalities by that herd.[8]

However, a linear model is likely a poor description of feedlot entry. Feedlots are sparse, and 86% of Brazilian municipalities gained none between 2004 and 2024. In addition, I expect exposure to raise entry in proportion to a municipality's cattle base. My preferred specification is therefore the exponential counterpart of equation (7),

$$\mathbb{E}\left[\Delta Y_i \mid C_i, \mu_i, X_i\right] = \exp\left(\alpha + \beta\, C_i + \gamma\, \mu_i + X_i'\delta\right), \tag{8}$$

which I estimate by Poisson pseudo-maximum likelihood (PPML) with the outcome in levels (Santos Silva and Tenreyro 2006). The estimator accommodates zeros and is consistent whenever the conditional mean is correctly specified. Here β is a semi-elasticity: one additional Mt-year of exposure multiplies expected feedlot growth by e^{β}.[9] All specifications include the same predetermined controls X_i: latitude, longitude, log land area, and the 2000 to 2004 averages of the log cattle herd and the pasture share of land area.

The coefficient β measures how much more feedlot capacity a municipality built because the plants near it were authorized earlier, and therefore faced more Chinese demand, than its location alone would predict. It is identified from municipalities near plants in the two queues, since a municipality far from every candidate plant sees $\tilde{C}_i$ near zero under any assignment. It is also a relative effect, since any consequence of Chinese demand that reaches all Brazilian producers alike, for example through the national price of cattle, is absorbed by the constant. Finally, because I observe the feedlots that operate in 2024, β measures the response of capacity that was built after 2004 and survived, which is the object that the accounting in Section 5 requires.

Results. I first examine whether recentered exposure behaves as the design requires. If the assignment process is correctly specified, recentered exposure should be unrelated to municipality characteristics determined before the first authorization. I test this by comparing the correlation of $\tilde{C}_i$ with each characteristic against the correlations produced by 10,000 alternative assignments (Table A3 in Appendix C). Recentered exposure is unrelated to latitude, longitude, land area, the baseline herd, and the baseline pasture share. No correlation exceeds 0.06 in absolute value, the randomization p-values range from

[8] Without weights, the per-head outcome is dominated by municipalities with very small herds, where a single feedlot produces an extreme rate.

[9] This specification goes one step beyond BH, who discuss nonlinear outcome models for the recentered instrument. In addition to the assumption of the correctly modeled assignment process, this approach requires that the assumed exponential form of the conditional mean is correctly specified.

0.51 to 0.92, and a joint test does not reject balance ($p = 0.86$). The queues matter for this result: when I permute authorization years across all nominated plants as a single pool, the same joint test rejects ($p = 0.01$). At the plant level, the timing of authorization within a queue is unrelated to whether a plant belongs to one of the three largest meatpacking firms ($p = 0.85$), to its location, and to its slaughter capacity.

Recentered exposure is, however, still correlated with expected exposure in my sample (0.32). A correlation of this size is not unusual under the assignment process ($p = 0.34$), so it is not evidence against the design. It does mean that, in this realization, municipalities with favorable timing also tended to have many candidate plants nearby. The recentered IV is exposed to this imbalance: its first-stage coefficient is 1.45, where it would be one if the two components were unrelated. The controlled specifications remove the imbalance by holding μ_i fixed. For this reason, and following the recommendation of BH, I put more weight on equations (7) and (8) than on the IV.

Table 2 reports the estimates. Columns 1 and 4 relate feedlot growth to realized exposure without adjustment, and Columns 2, 3, and 5 use the recentered design. In my preferred specification (Column 5), one additional Mt-year of exposure raises the number of feedlots built after 2004 by 23% and the pen area added by 21%. The linear specifications give a similar answer. The controlled OLS estimate of 0.18 feedlots per 100,000 head is 20% of the mean of the outcome, and the estimate for pen area is 21% of its mean. The recentered IV estimates are somewhat smaller, at 16% and 17%. That the number and the area of feedlots respond in the same proportion indicates that exposure led to more feedlots but not to larger ones. Applied to the distribution of realized exposure, the estimate implies 3.8 times as many feedlots built over the sample period for a one-standard-deviation increase in exposure.

The unadjusted coefficients in Columns 1 and 4 are about one third as large as the recentered ones. Because expected exposure accounts for nearly all of the variation in realized exposure, the unadjusted regressions mostly compare regions with many and few candidate plants, and feedlot growth rises more slowly along that margin. This could reflect other characteristics of those regions, which is the selection that the design removes, or a response that flattens at high levels of exposure, to which I return below.

The standard errors in parentheses allow for spatial correlation among municipalities within 300 km of each other. I also report randomization inference p-values in brackets, which BH propose for this situation and which are valid even in experiments with a relatively small number of shocks. The test asks a simple question: if exposure had no effect on any municipality, how often would the assignment process alone produce an association between recentered exposure and feedlot growth as strong as the one I observe? To answer it, I hold outcomes fixed, redraw the authorization years within queues 10,000 times, and recompute recentered exposure for each draw. The p-value is the share of draws in which

TABLE 2. Effect of exposure to Chinese demand on feedlot growth, 2004 to 2024

	Linear, per 100,000 head			PPML	
	OLS	Recentered IV	Controlled OLS	Unadjusted	Controlled
	(1)	(2)	(3)	(4)	(5)
A. Number of feedlots					
Exposure, C_i	0.060	0.140	0.181	0.055	0.207
	(0.017)	(0.038)	(0.041)	(0.012)	(0.042)
		[0.010]	[0.020]		[0.023]
Mean of outcome	0.89	0.89	0.89	0.30	0.30
Implied semi-elasticity	0.07	0.16	0.20	0.05	0.21
B. Pen area (hectares)					
Exposure, C_i	0.651	1.318	1.666	0.068	0.194
	(0.164)	(0.388)	(0.427)	(0.013)	(0.052)
		[0.020]	[0.044]		[0.047]
Mean of outcome	7.84	7.84	7.84	2.65	2.65
Implied semi-elasticity	0.08	0.17	0.21	0.07	0.19
Control for μ_i	No	No	Yes	No	Yes
Municipalities	5,530	5,530	5,530	5,563	5,563

Notes: Each column reports the coefficient on cumulative exposure to Chinese demand, in Mt-years. The outcome is the change from 2004 to 2024 in the count of feedlot facilities (Panel A) or in their pen area (Panel B). In Columns 1 to 3, the outcome is divided by the municipality's 2000 to 2004 cattle herd, and municipalities are weighted by that herd. Column 2 instruments exposure with recentered exposure, and Columns 3 and 5 control for expected exposure. Columns 4 and 5 are estimated by Poisson pseudo-maximum likelihood with the outcome in levels. All columns control for latitude, longitude, log land area, the log of the 2000 to 2004 cattle herd, and the 2000 to 2004 pasture share. Standard errors in parentheses allow for spatial correlation within 300 km. Randomization inference p-values for the null of no effect, from 10,000 permutations of authorization years within nomination queues, are in brackets.

the covariance between redrawn exposure and feedlot growth, net of the controls, is at least as large in absolute value as the realized one.[10] In the preferred specification, the test rejects the null of no effect for both outcomes ($p = 0.023$ for feedlots and $p = 0.047$ for pen area), and the linear specifications give similar or smaller p-values. In other words, feedlot growth lines up with the order in which China actually authorized plants more closely than with all but a few percent of the orders it could have chosen within the same queues. Inverting the test for the controlled OLS gives a 95% confidence interval of 0.04 to 0.34 feedlots per 100,000 head.

Appendix C reports alternative specifications. The PPML estimates lie between 0.18 and 0.21 for feedlots and between 0.18 and 0.19 for pen area across specifications that account for the baseline herd, whether as a control, with its coefficient fixed at one, or together with the 2004 stock of feedlots. Without any adjustment for the herd, the estimates

[10] For the PPML, I use the score form of the statistic that Borusyak and Hull (2021) derive for nonlinear models: the covariance between recentered exposure and the residual from the model estimated without exposure.

range from 0.12 to 0.22 and are imprecise. The linear estimates are also positive but less precise when the outcome is not scaled by the herd. In addition, no single plant drives the result. Every estimate obtained by removing one plant at a time from recentered exposure is positive, with a Conley t-statistic above 2.9 for feedlots and 2.7 for pen area, and randomization p-values no larger than 0.03 for feedlots and 0.05 for pen area.

5 A Land-Use Counterfactual

The reduced-form estimates in Section 4.5 indicate that exposure to the Chinese market increased feedlot capacity. In this section, I use those estimates to quantify what the induced shift toward confined finishing implied for the amount of pasture required to produce Brazilian beef, and for the carbon stored on that land. To do so, I combine the estimates with cattle-movement records, land-cover data, and parameters calibrated from industry benchmarks in a spatial accounting exercise. The goal of this exercise is to use the reduced-form estimates to inform a credible back-of-the-envelope calculation rather than develop a structural model of the beef industry. Each calibration step relies on the best data available to me, and I report a central estimate along with its sensitivity to the main alternative choices. Appendix D documents each step in more detail.

Overview. Confined finishing reduces pasture requirements primarily because cattle spend less time grazing before slaughter. Under the traditional production system, a Brazilian beef animal is born and reared on pasture and remains there until it reaches slaughter weight, which typically occurs at 30 months of age or more. In a feedlot system, the same animal is moved off pasture at an average age of 23 months, fed a grain-based ration in confinement for several months, and slaughtered at an average of 26 months with a somewhat heavier market weight. Holding the quantity of beef produced fixed, this changes pasture requirements through two channels. First, each animal grazes for fewer months before slaughter. Second, because each feedlot-finished animal yields a heavier carcass, fewer animals are needed to produce a given quantity of beef. Both channels reduce the total number of animal-months spent on pasture, which, at a given stocking density, translates directly into fewer hectares of pasture.

The counterfactual I consider asks how much additional pasture would have been required to produce Brazil's 2024 beef output if the feedlot capacity attributable to Chinese export access had not been built, and the cattle finished in that capacity had instead been brought to market using the production practices observed in pasture-based systems today. I hold fixed total beef output, the feedlot capacity that is not attributable to China, the sourcing relationships between feedlots and the ranches that supply them, and the stocking density of pasture. I do not allow prices or quantities to adjust in response to the

removal of this capacity. Importantly, this means that the exercise does not speak to the scale effect of Chinese demand, that is, to the extent to which Brazil produced more total beef due to this export exposure shock. It instead isolates the technique effect, the shift in finishing technology that my reduced-form estimates attribute to export exposure, and quantifies what that shift implied for aggregate land use and associated emissions.

To frame the approach more precisely, let A^P denote the slaughter age of a pasture-finished animal, A^F the age at which a feedlot-finished animal enters confinement, and r^w the ratio of carcass weight per head under feedlot and pasture finishing. Producing one feedlot-finished animal's worth of beef on pasture requires r^w pasture-finished animals, each of which grazes for A^P months, in place of a single animal that grazes for A^F months. The additional grazing land requirement per feedlot-finished animal is therefore

$$r^w A^P - A^F = \underbrace{\left(A^P - A^F\right)}_{\text{grazing channel}} + \underbrace{\left(r^w - 1\right)A^P}_{\text{yield channel}} \tag{9}$$

Scaling this gap by the average stocking density of the surrounding pasture converts this quantity into hectares of pasture per animal, and multiplying by the number of cattle finished per hectare of pen each year yields the pasture requirement per hectare of feedlot capacity. Using the parameter values I calibrate below, the gap in equation (9) is approximately 9.3 animal-months, of which 7.8 reflect the shorter time on pasture and 1.5 reflect the heavier carcass. At the stocking densities prevailing in the regions that supply feedlot cattle, this amounts to roughly 0.45 hectares per head. By combining my feedlot panel with industry estimates of cattle finished in confinement in Brazil, I estimate that one hectare of pen capacity supports approximately 320 head per year nationally, with state rates that range from roughly 270 head in Goiás to 390 in São Paulo. Together, these figures imply that each hectare of feedlot capacity substitutes for roughly 146 hectares of pasture. This ratio is the key input into the counterfactual exercise.

I implement the counterfactual in five steps. First, I use the estimates from Section 4.5 to assign each municipality the share of its feedlot capacity that is attributable to exposure to the Chinese market, following the approach of Donaldson and Hornbeck (2016) in applying an estimated proportional response to each unit's observed level of exposure. Second, I convert this attributable pen area into a quantity of cattle finished per year using national and state-level industry estimates of confined-cattle throughput. Third, I use cattle-movement records to trace these cattle back to the municipalities that supplied them. Fourth, I convert the cattle into hectares of pasture using the ages, carcass weights, and stocking densities described above. Finally, I use each municipality's historical pattern of pasture expansion to determine the land-cover types from which this additional pasture would likely have been drawn, and I quantify the carbon stored in that land using Brazil's national greenhouse gas inventory.

Approach. The first step assigns each municipality with feedlots, indexed by f, the share of its pen area that is attributable to Chinese market access. Let P_f be the pen area the municipality added between 2004 and 2024, the outcome of equation (8), which models its conditional mean as

$$\bar{P}_f \equiv \mathbb{E}\left[P_f \mid C_f, \mu_f, X_f\right] = \exp\left(\alpha + \beta C_f + \gamma \mu_f + X_f'\delta\right),$$

where C_f is the municipality's cumulative exposure, μ_f its expected exposure, and X_f the controls. Let P_f^0 be the pen area the municipality would have added with no exposure to the Chinese market. Under the model, its conditional mean is the same expression with C_f set to zero and everything else held fixed,

$$\bar{P}_f^0 = \exp\left(\alpha + \gamma \mu_f + X_f'\delta\right) = e^{-\beta C_f}\,\bar{P}_f,$$

so exposure scales expected pen area by $e^{\beta C_f}$ and changes nothing else. The expected pen area attributable to exposure is the difference $\bar{P}_f - \bar{P}_f^0$, which as a share of expected pen area is

$$s_f = \frac{\bar{P}_f - \bar{P}_f^0}{\bar{P}_f} = 1 - e^{-\beta C_f}, \tag{10}$$

where $\beta = 0.194$ per Mt-year is the estimate for pen area in Column 5 of Table 2. Since exposure is never negative, s_f lies between zero and one.

I multiply s_f by the pen area that each municipality actually added over the period. The regression describes the average municipality at a given level of exposure, so this step assumes that the proportional effect holds municipality by municipality: a place that built more than the regression predicts, for reasons the regression does not capture, would also have built proportionally more without China.[11] The step is similar in spirit to Donaldson and Hornbeck (2016), who multiply each county's predicted percentage loss in land value from removing the railroads by the county's actual land value. The attraction of applying the share to actual rather than predicted pen area is that the counterfactual removes capacity only where it currently exists. Municipalities without feedlots are untouched, no capacity is moved between municipalities, and the cattle removed in each place can be traced to the municipalities that supplied them in the next step. Sites that were already in operation in 2004 predate the first authorization and are assigned no attributable share. Aggregating across municipalities, 8,794 hectares of pen area are attributable to Chinese market access, corresponding to 60% of the pen area added since 2004.

Converting pen area into cattle requires distinguishing between a stock and a flow,

[11] Equation (10) also extrapolates the estimated response across the full range of observed exposure, whereas the variation that identifies β comes from the timing of authorization within a queue and shifts a municipality's exposure by at most a few megatonne-years. I treat the constant semi-elasticity as a maintained assumption.

as a pen holds a single lot of animals at a time and is typically turned over several times per year. The industry census of confinement reports the number of cattle finished in Brazilian feedlots each year, which reached 7.96 million head in 2024. I divide the growth in this count since 2004 by the growth in detected pen area over the same period, which yields approximately 321 head per hectare per year. Throughput per hectare of pen is not uniform across the country, however, since feedlots differ in how many lots of cattle they finish in a year. The census also publishes state totals for the five largest feedlot states, and these imply that São Paulo finishes the most cattle per hectare of detected pen area and Goiás the fewest. I therefore scale the national rate by each of these states' throughput relative to the others, normalized so that the five states together reproduce the national rate, which gives between 272 head per hectare in Goiás and 386 in São Paulo, and I apply the national rate in the remaining states (Appendix D.2). This implies that approximately 2.87 million head, or 36% of all cattle confined in 2024, were finished in capacity attributable to Chinese market access.

Because feedlots often source cattle from ranches located far away (Figure A9), the pasture that a feedlot replaces is generally not located in the feedlot's own municipality. To trace the attributable cattle back to their origins, I use animal transit permits (GTA), which accompany cattle shipments in Brazil and record the origin and destination municipality, the purpose of the shipment, and the sex and age bracket of the animals shipped. Three states publish these records: Mato Grosso, Pará, and Espírito Santo. Using shipments of male cattle for finishing into municipalities with feedlots, I estimate a gravity-style regression in which the number of cattle that a feedlot municipality sources from each origin within its state is increasing in the origin's herd and pasture area, decreasing in road distance, and higher for the feedlot's own municipality. The fitted model provides, for every feedlot municipality in Brazil, the share of its cattle sourced from each potential origin, and I use these shares to allocate the attributable cattle upstream. Weighted by pen area, the predicted sourcing pattern implies that a feedlot draws roughly 26% of its cattle from its own municipality and roughly one third from within 100 km, with a mean sourcing distance of 234 km. In total, the allocation reaches 5,185 municipalities.

Three parameters are needed to convert the attributable cattle into hectares of pasture. The age at feedlot entry, 22.6 months, is the average entry age for bulls reported in a 2023 survey of feedlot nutritionists, whose clients accounted for approximately 80% of the cattle finished in confinement in Brazil that year (Monsalve and Millen 2025). The slaughter age of pasture-finished cattle, 30.4 months, is calculated from transit permits for slaughter shipments of male cattle originating in municipalities with no feedlots. The carcass ratio, 1.05, compares the average carcass weight of feedlot-finished cattle reported in an industry benchmarking survey (306 kg) with the carcass weight implied for the remaining male cattle by the national slaughter statistics (291 kg). I restrict all three parameters to males

for two reasons. Roughly 90% of feedlot-finished cattle in Brazil are male, whereas cows account for a substantial share of pasture-based slaughter and are both lighter and older at slaughter for reasons unrelated to the finishing system. Comparing feedlot cattle with all pasture-finished cattle would therefore conflate differences in herd composition with the productivity gains from confined finishing. Finally, I measure stocking density as the municipal cattle herd divided by municipal pasture area, averaged over 2020 to 2023, so that the counterfactual cattle are raised using current pasture-based practices. Because cattle standing in pens inflate the measured density of municipalities with feedlots, those municipalities are assigned the density of neighboring municipalities without feedlots.

Because stocking density is held fixed, each additional animal-month requires additional pasture, and the final step is to determine what land cover this pasture would have replaced. The MapBiomas land-cover maps record annual transitions into pasture for each municipality since 2004, which allows me to characterize the land-cover types from which each municipality's pasture has historically expanded. I allocate each municipality's counterfactual pasture across these classes in proportion to its historical transitions, subject to the constraint that the allocation cannot exceed the area of each class remaining in the municipality in 2023. I then value the carbon stored in the converted land using per-hectare carbon stocks from Brazil's Fourth National Greenhouse Gas Inventory, which vary by land-cover class and biome and include above- and below-ground biomass, litter, and dead wood, but exclude soil carbon. I net out the carbon stock of the pasture that replaces each class. The resulting quantity is the carbon stock standing on the land that the counterfactual pasture would have displaced, which I interpret as a potential carbon loss under the counterfactual. For example, converting cropland to pasture releases essentially no carbon under this measure, whereas converting a hectare of Amazon forest releases approximately 155 tonnes of carbon.

Results. Table 3 summarizes the main results, and Figure 11 maps the spatial distribution of the counterfactual pasture requirement. Finishing the 2.87 million attributable cattle on pasture would have required approximately 1.29 million hectares of additional pasture, which exceeds the observed total expansion of Brazil's pasture area between 2004 and 2024. The spatial distribution of this requirement follows the location of feedlots and their sourcing areas. Mato Grosso, Goiás, São Paulo, Mato Grosso do Sul, and Minas Gerais together account for 84% of the total. The municipalities with the largest requirements are major cattle-producing municipalities that supply the feedlot belt extending from Goiás through Mato Grosso do Sul to western São Paulo.

Most of the land that this pasture would have displaced is not forest. Based on historical transition patterns, 39% of the counterfactual pasture would be drawn from the mosaic of small-scale agriculture and pasture, 16% from cropland, 20% from savanna, and 20% from

TABLE 3. Pasture and carbon under the counterfactual

A. National	
Feedlot pen area in 2024 (hectares)	14,935
Pen area attributable to exposure (hectares)	8,794
Share of pen area added since 2004	0.60
Cattle finished in the attributable pens (million head per year)	2.87
Share of cattle confined in 2024	0.36
Additional pasture (million hectares)	1.29
Percent of pasture area in 2023	0.82
Hectares per head	0.45
Hectares per hectare of pen	146
From forest formation (million hectares)	0.25
From savanna formation	0.26
From cropland and the mosaic of farms and pasture	0.70
From grassland, other native vegetation, and planted forest	0.07
Carbon stock on the converted land, net of pasture (Mt C)	46.0
In CO_2 (Mt)	169
Of which forest formation	124
Of which savanna formation	39
Cropland growing feed for the attributable cattle (million hectares)	0.42

B. By state

	Attributable pen area (ha)	Cattle (thousand head)	Additional pasture (thousand ha)	Of which forest (thousand ha)	CO_2 (Mt)
Mato Grosso	1,725	546	290	82	60.4
Goiás	1,752	475	182	15	10.2
São Paulo	2,116	815	255	2	2.5
Mato Grosso do Sul	1,081	335	174	29	15.1
Minas Gerais	929	309	176	9	5.6
Pará	366	117	86	75	46.9
Tocantins	351	113	66	14	12.0
Rondônia	205	66	25	22	13.2
Other states	269	86	34	5	2.8
Total	8,794	2,861	1,287	254	168.6

Notes: Panel A reports the central estimate of the counterfactual described in the text. Pen area attributable to exposure applies equation (10) to the pen area each municipality added between 2004 and 2024. Cattle are the attributable pen area times the state's rate of cattle finished per hectare of pen per year (Appendix D.2). Additional pasture is the pasture needed to finish those cattle on grass. Carbon is the Fourth National Inventory stock of the source class in the municipality's biome, net of the pasture stock, excluding soil. Panel B reports state-level estimates.

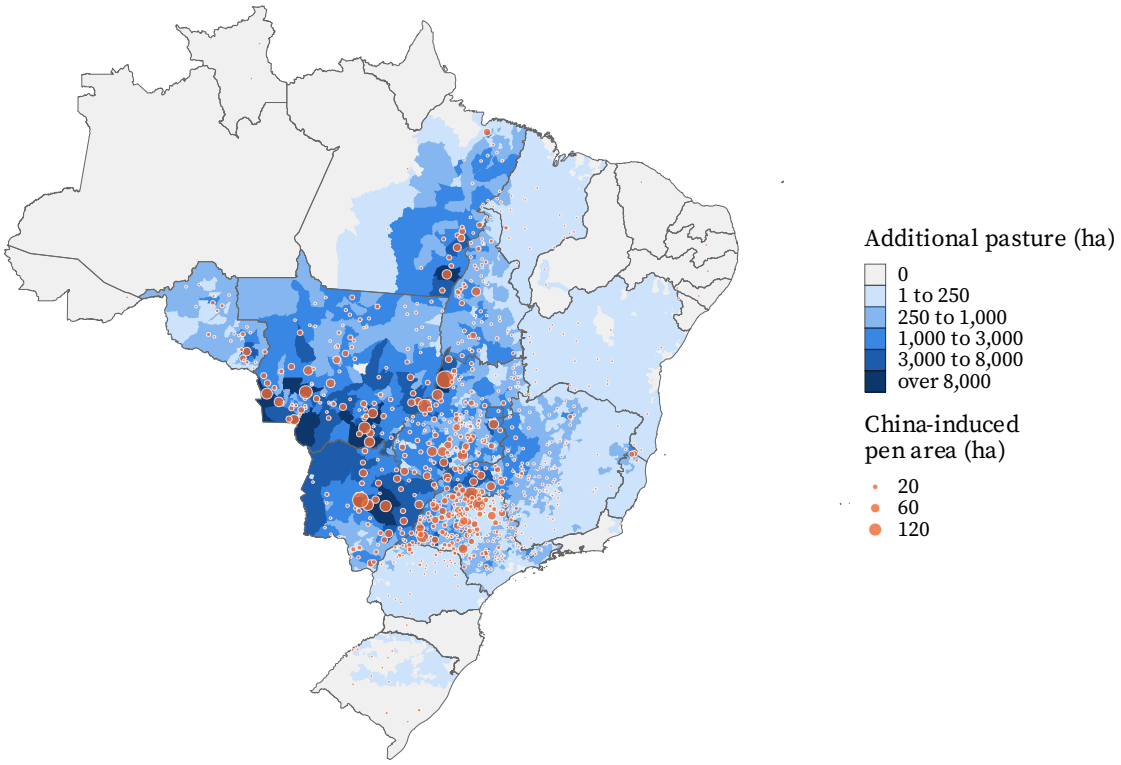


FIGURE 11. Counterfactual pasture requirement

Notes: Shading gives the additional pasture required in each municipality, in hectares, to finish on grass the attributable feedlot cattle that the municipality supplies. Circles mark municipalities with feedlots, with area proportional to the pen area attributable to exposure. Cattle are allocated from feedlot municipalities to the municipalities that supply them with the sourcing weights estimated from transit permits.

forest formation. However, the carbon implications are concentrated almost entirely in the forest and savanna components. The 1.29 million hectares hold approximately 46.0 million tonnes of carbon net of pasture, equivalent to 169 million tonnes of CO_2. Forest formation accounts for 73% of this total despite representing only one fifth of the converted area, and savanna accounts for a further 23%. By biome, the Amazon contributes 0.22 million hectares but 66% of the carbon, while the Cerrado contributes 0.69 million hectares and 26%. Panel B of Table 3 illustrates the same pattern across states. São Paulo has the largest attributable pen area and sources the largest number of cattle, but its additional pasture would be drawn primarily from cropland and accounts for only 2.5 million tonnes of CO_2. In contrast, Mato Grosso and Pará, where pasture expansion has historically come at the expense of forest, together account for 64% of the carbon.

Feedlot-finished cattle also consume crops, so part of the pasture saving from confined finishing is offset by the cropland required to produce feed. According to the 2023 nutritionist survey, feedlot cattle spend an average of 106 days on feed and consume 10.75 kg of dry matter per day, with maize grain accounting for 54% of the diet, roughage (mostly maize silage) for 16%, and soybean meal for roughly 2%. At national average yields for 2022 to 2024, this corresponds to approximately 0.15 hectares of cropland per animal, or 0.42 million hectares for the attributable cattle, roughly one third of the pasture requirement. Netting the two implies an additional land requirement of 0.87 million hectares. I report the feed-crop land as a national aggregate only, as I am not able to allocate it to the municipality level in my current framework. However, feed crops are predominantly produced in the Center-West and South regions of Brazil, which generally have lower carbon density per hectare than frontier regions. Appendix D.8 provides additional details for this calculation.

The central estimate is relatively insensitive to the choice of reduced-form specification but more sensitive to two of the calibrated parameters (Appendix D.9). Using the four alternative estimates of β reported in Appendix C yields additional pasture requirements between 1.23 and 1.32 million hectares and carbon losses between 160 and 174 million tonnes of CO_2. The yield ratio and the age assigned to the oldest bracket of pasture-finished cattle have larger effects. If I assume no yield premium, the pasture requirement falls to 1.08 million hectares, while the highest premium reported in the industry data raises it to 1.75 million hectares, and the two alternative values for the oldest age bracket imply 1.19 and 1.59 million hectares. Given this range, I interpret the central estimate as an order of magnitude rather than as a precise value: the technique effect of China-induced feedlot adoption amounts to over one million hectares of pasture and between 150 and 200 million tonnes of CO_2.

Discussion. This exercise quantifies one margin of the relationship between export demand and land use, and several limitations should be kept in mind when interpreting the results. Most importantly, the counterfactual does not address the scale effect. Chinese demand likely increased total Brazilian beef production, and higher output requires more pasture; the technique effect quantified here offsets part of that increase, but I do not estimate the scale effect and therefore cannot characterize the net effect of Chinese demand on pasture area. In addition, the counterfactual holds both the sourcing network and the feedlot capacity not attributable to China fixed. The map should therefore be interpreted as showing where the pasture replaced by the attributable feedlots would have been grazed under the existing sourcing patterns, rather than as a precise prediction of where deforestation would have occurred. If feedlots relocated toward more exposed municipalities rather than representing net additions to national capacity, the aggregate figure overstates the capacity created by exposure, whereas if Chinese demand increased feedlot entry everywhere through higher cattle prices, it likely understates it.

This exercise falls well short of a full accounting of the environmental costs and benefits of confined finishing. Feedlots concentrate manure, with consequences for local water quality, and require the transport of cattle and feed over long distances; I do not account for either, and feed-crop land enters only as a national aggregate. One omission whose direction can be signed is enteric methane. Life-cycle studies consistently find that greenhouse gas emissions per kilogram of beef are lower in concentrate-based finishing systems than in roughage-based systems, so omitting methane does not reverse the direction of the technique effect quantified here.[12]

6 Conclusion

In this paper, I focus on Brazil's beef export boom to China and the expansion of confined cattle finishing. After processing plants gain access to the Chinese market, they increasingly source younger cattle and draw more heavily from municipalities with feedlots. Feedlot entry also rises in the regions surrounding newly authorized plants. These patterns remain when I use the timing and institutional structure of the authorization process to address omitted variables affecting the probability of export authorization and reverse causality. Taken as a whole, the results imply that a substantial share of the feedlot capacity operating in Brazil today is attributable to the growth in exposure to the Chinese market.

[12] de Vries, van Middelaar, and de Boer (2015) review 14 life-cycle assessments comparing beef production systems and find that global warming potential per unit of beef is approximately 28% lower in concentrate-based than in roughage-based systems, largely because animals reach slaughter weight more quickly. Methane emissions from feedlot-finished cattle are therefore not higher per unit of output, and the pasture and carbon margin I quantify here is not offset by higher enteric emissions.

This technological response matters for land use because feedlot finishing changes how long cattle spend on pasture. Holding beef output fixed, moving cattle into confinement for the final stage of production reduces the stock of animals grazing at any point in time and, because feedlot-finished cattle are heavier at slaughter, reduces the number of animals required to produce a given quantity of beef. Combining the reduced-form estimates with industry benchmarks and cattle-movement data, I estimate that producing current output without the feedlot capacity attributable to China would require approximately 1.29 million additional hectares of pasture, implying roughly 169 $MtCO_2$ in potential carbon losses under historical land-conversion patterns. These calculations are best interpreted as an order of magnitude benchmark to compare with other drivers of land-use change in this context, but they nonetheless suggest that the technique response to export demand had meaningful land-sparing effects.

This distinction matters for how the environmental effects of agricultural trade are evaluated. Policies aimed at removing deforestation from commodity supply chains, such as the European Union Deforestation Regulation, require firms to trace cattle through the establishments where they were raised and demonstrate that production is not linked to land deforested after 2020. Such policies target an important externality, but observed deforestation embodied in an export supply chain does not identify the full effect of export demand on land use. The same demand shock that raises returns to expanding production can also raise returns to technologies that lead to higher productivity and, ultimately, more efficient land use. This does not imply that deforestation restrictions are fully misguided, but it does suggest that evaluating these policies requires accounting for both margins of production adjustment to increased international demand.

My results also add nuance to the land-sparing versus land-sharing debate (Phalan, Onial, Balmford et al. 2011). Confined finishing is more industrial and spatially concentrated than pasture finishing, and it requires additional cropland for feed. In my accounting, producing feed for the China-attributable cattle requires roughly one third of the pasture area saved. But the location and type of land matter greatly for total emissions accounting. An additional hectare of maize on existing agricultural land is not environmentally equivalent to an additional hectare of pasture expanding into native forest at the agricultural frontier. The carbon consequences in my counterfactual are concentrated in those frontier regions. Intensive livestock production can therefore impose additional local land requirements while still reducing pressure on land elsewhere in the supply chain.

There are several limits to what these estimates establish. The satellite data identify a lower bound on current feedlot capacity and recover historical growth from the opening dates of facilities that remain observable today. More importantly, the counterfactual isolates the technique effect and says nothing about the scale effect of Chinese demand. I

also cannot fully distinguish new national feedlot capacity from capacity that may have developed elsewhere or later in the absence of Chinese demand. The results are therefore most informative about the acceleration and spatial allocation of technological change induced by export access, rather than the complete general-equilibrium effect of China on Brazilian cattle production. Finally, this is not a full environmental or welfare accounting. Feedlots create local externalities, including manure and water-quality concerns, and raise animal-welfare questions outside the scope of this paper.

The broader point is that production technology is endogenous to market access. Agricultural trade changes where and how much is produced, but it can also change how production is organized. Accounting for that response is necessary for understanding the environmental consequences of trade, particularly in land-intensive sectors where changes in production technique can translate into large changes in land demand.

References

ABIEC. 2024. "Brazilian Beef Exports and Domestic Consumption Report 2024." https://www.abiec.com.br/wp-content/uploads/beefreport_v2024-ENG.pdf. Statistics on proportion of beef output consumed domestically vs exported in Brazil in 2023.

Aires, Uilson R. V., Vitor S. Martins, Dakota J. Hester, Thainara M. A. Lima, and Lucas B. Ferreira. 2026. "National-scale open cattle feedlot detection using deep learning and high-resolution aerial images: Spatial distribution and animal welfare analysis." *Science of The Total Environment* 1015: 181451. 10.1016/j.scitotenv.2026.181451.

Amodio, Francesco, Giorgio Chiovelli, and Serafín Frache. 2025. "Beefing Up the Service Sector: Commodity Exports to China and Production Network Spillovers." https://economics.yale.edu/sites/default/files/2025-03/Beefing%20Up%20the%20Service%20Sector_0.pdf. Working paper.

AQSIQ and MAPA. 2015. "Protocolo entre a Administração Geral de Supervisão da Qualidade, Inspeção e Quarentena da República Popular da China e o Ministério da Agricultura, Pecuária e Abastecimento da República Federativa do Brasil em Relação às Condições de Quarentena e Sanitárias Veterinárias da Carne Bovina a Ser Exportada do Brasil para a China." https://www.cebc.org.br/sites/default/files/protocolo_entre_aqsiq_e_mapa_em_relacao_as_condicoes_de_quarentena_e_sanitarias_veterinarias_da_carne_bovina_a_ser_exportada_do_brasil_para_a_china.pdf. Bilateral sanitary protocol.

Assunção, Juliano, Robert McMillan, Joshua Murphy, and Eduardo Souza-Rodrigues. 2023. "Optimal Environmental Targeting in the Amazon Rainforest." *The Review of Economic Studies* 90 (4): 1608–1641. 10.1093/restud/rdac064.

Bai, Jushan and Pierre Perron. 1998. "Estimating and Testing Linear Models with Multiple Structural Changes." *Econometrica* 66 (1): 47–78. 10.2307/2998540.

Borusyak, Kirill and Peter Hull. 2021. "Non-Random Exposure to Exogenous Shocks: Theory and Applications." Working Paper 27845, National Bureau of Economic Research.

Borusyak, Kirill and Peter Hull. 2023. "Nonrandom Exposure to Exogenous Shocks." *Econometrica* 91 (6): 2155–2185. 10.3982/ECTA19367.

Bustos, Paula. 2011. "Trade Liberalization, Exports, and Technology Upgrading: Evidence on the Impact of MERCOSUR on Argentinian Firms." *American Economic Review* 101 (1): 304–340. 10.1257/aer.101.1.304.

Bustos, Paula, Bruno Caprettini, and Jacopo Ponticelli. 2016. "Agricultural Productivity and Structural Transformation: Evidence from Brazil." *American Economic Review* 106 (6): 1320–1365. 10.1257/aer.20131061.

Callaway, Brantly and Pedro H. C. Sant'Anna. 2021. "Difference-in-Differences with Multiple Time Periods." *Journal of Econometrics* 225 (2): 200–230. 10.1016/j.jeconom.2020.12.001.

Cargill. 2024. "Benchmarking Confinamento Probeef, 8a edição." https://www.cargill.com.br/pt_BR/2025/benchmarkingconfinamento25.

Carleton, Tamma, Levi Crews, and Ishan Nath. 2025. "Agriculture, Trade, and Global Water Use." https://www.levicrews.com/files/p-wateruse_paper.pdf. Working paper.

Conley, Timothy G. 1999. "GMM Estimation with Cross Sectional Dependence." *Journal of Econometrics* 92 (1): 1–45.

Copeland, Brian R. and M. Scott Taylor. 2004. "Trade, Growth, and the Environment." *Journal of Economic Literature* 42 (1): 7–71. 10.1257/002205104773558047.

Cruz, José Carlos. 1998. "Cultivares de milho para silagem." In *Congresso Nacional dos Estudantes de Zootecnia*. Viçosa: Embrapa Milho e Sorgo.

de Vries, M., C.E. van Middelaar, and I.J.M. de Boer. 2015. "Comparing environmental impacts of beef production systems: A review of life cycle assessments." *Livestock Science* 178: 279–288. https://doi.org/10.1016/j.livsci.2015.06.020.

Dell, Melissa. 2025. "Deep Learning for Economists." *Journal of Economic Literature* 63 (1): 5–58. 10.1257/jel.20241733.

Dias, Fabio Martins Guerra Nunes, Fredson Vieira e Silva, AndréGuimarães Maciel e Silva, Guilherme Jordão de Magalhães Rosa, and JoséBento Sterman Ferraz. 2025. "Logistics and CO2e emissions from beef cattle transportation in Brazil between 2018 and 2020." *Scientific Reports* 15 (1): 38063.

Domínguez-Iino, Tomás. 2025. "Efficiency and Redistribution in Environmental Policy: An Equilibrium Analysis of Agricultural Supply Chains." *Journal of Political Economy* .

Donaldson, Dave and Richard Hornbeck. 2016. "Railroads and American Economic Growth: A "Market Access" Approach." *Quarterly Journal of Economics* 131 (2): 799–858. 10.1093/qje/qjw002.

dsm-firmenich. 2025. "Censo Confinamento Brasil 2025." https://www.dsm-firmenich.com/content/dam/dsm/tortuga/pt_BR/documents/DSM_CENSO_CONFINAMENTO_2025.pdf. Annual industry census of cattle confinement.

Farrokhi, Farid, Elliot Kang, Heitor S. Pellegrina, and Sebastian Sotelo. 2025. "Deforestation: A Global and Dynamic Perspective." Working Paper 34150, National Bureau of Economic Research, Cambridge, MA. 10.3386/w34150.

Figueiredo, Nayara. 2022. "Brazil increases feedlots use to meet China importing requirements." *Reuters* https://www.reuters.com/business/brazil-increases-feedlots-use-meet-china-importing-requirements-2022-04-05/.

Food and Agriculture Organization of the United Nations. 2022. "The State of Agricultural Commodity Markets 2022: The Geography of Food and Agricultural Trade: Policy Approaches for Sustainable Development."

General Administration of Customs of the People's Republic of China. 2021. "Regulations of the People's Republic of China on the Registration and Administration of Overseas Producers of Imported Food." https://www.mofcom.gov.cn/zcfb/zgdwjjmywg/art/2021/art_b086bef4f0d14d1d8a9469ff70f63259.html. Decree No. 248, issued April 12, 2021; effective January 1, 2022.

Khachiyan, Arman, Anthony Thomas, Huye Zhou, Gordon Hanson, Alex Cloninger, Tajana Rosing, and Amit K. Khandelwal. 2022. "Using Neural Networks to Predict Microspatial Economic Growth." *American Economic Review: Insights* 4 (4): 491–506. 10.1257/aeri.20210422.

MapBiomas Project. 2025. "Collection 10 of the Annual Land Use and Land Cover Maps of Brazil." https://mapbiomas.org/. Accessed on 2025-08-28.

Marx, Benjamin, Thomas M. Stoker, and Tavneet Suri. 2019. "There Is No Free House: Ethnic Patronage in a Kenyan Slum." *American Economic Journal: Applied Economics* 11 (4): 36–70. 10.1257/app.20160484.

Mello, Renius, José Laerte Nörnberg, Marta Gomes da Rocha, and Diego Bitencourt de David. 2005. "Características produtivas e qualitativas de híbridos de milho para produção de silagem." *Revista Brasileira de Milho e Sorgo* 4 (1): 79–94.

Ministério da Agricultura, Pecuária e Abastecimento. 2010. "Circular No. 596/2010/CGPE/DIPOA." Brasília, July 26, 2010. Obtained through an access-to-information request.

Mishra, Prakash. 2025. "The Global Allocative Efficiency of Deforestation." https://faculty.wharton.upenn.edu/wp-content/uploads/2019/08/PrakashMishra_JMP.pdf. Job market paper; draft dated January 1, 2025.

Moffette, Fanny, Marin Skidmore, and Holly K. Gibbs. 2021. "Environmental policies that shape productivity: Evidence from cattle ranching in the Amazon." *Journal of Environmental Economics and Management* 109: 102490.

Monsalve, Julia Gabrielle and Danilo Domingues Millen. 2025. "A Snapshot of Nutritional Recommendations and Management Practices Adopted by Feedlot Cattle Nutritionists in Brazil in 2023." *Frontiers in Veterinary Science* 12: 1518571. 10.3389/fvets.2025.1518571.

Pellegrina, Heitor S. 2022. "Trade, productivity, and the spatial organization of agriculture: Evidence from Brazil." *Journal of Development Economics* 156: 102816.

Phalan, Ben, Malvika Onial, Andrew Balmford, and Rhys E. Green. 2011. "Reconciling Food Production and Biodiversity Conservation: Land Sharing and Land Sparing Compared." *Science* 333 (6047): 1289–1291. 10.1126/science.1208742.

Poore, Joseph and Thomas Nemecek. 2018. "Reducing food's environmental impacts through producers and consumers." *Science* 360 (6392): 987–992.

Revista DBO. 2025. "Top 20 Confinadores 2025." *Revista DBO* https://portaldbo.com.br/top-20-confinadores-2025/.

Santos Silva, J. M. C. and Silvana Tenreyro. 2006. "The Log of Gravity." *Review of Economics and Statistics* 88 (4): 641–658.

Sayre, James E. 2026. "Farm to Firm: Clustering and Returns to Scale in Agricultural Supply Chains." http://jaysayre.com/docs/jesayre_farmtofirm.pdf. Working paper.

Scot Consultoria. 2024. “Boitel como estratégia lucrativa em confinamentos no MT.” *Scot Consultoria* https://www.scotconsultoria.com.br/noticias/todas-noticias/57776/.

SEEG. 2024. “Nota metodológica do Sistema de Emissões e Remoções de Gases de Efeito Estufa no Brasil (1990–2023): Mudanças de Uso da Terra e Florestas.” Tech. rep., Instituto de Pesquisa Ambiental da Amazônia (IPAM). Version 12, November 2024.

Shapiro, Joseph S. and Reed Walker. 2018. “Why Is Pollution from US Manufacturing Declining? The Roles of Environmental Regulation, Productivity, and Trade.” *American Economic Review* 108 (12): 3814–54. 10.1257/aer.20151272.

Silvestre, Antonio Marcos and Danilo Domingues Millen. 2021. “The 2019 Brazilian Survey on Nutritional Practices Provided by Feedlot Cattle Consulting Nutritionists.” *Revista Brasileira de Zootecnia* 50: e20200189. 10.37496/rbz5020200189.

Singh, Chandrakant and U. Martin Persson. 2026. “Global patterns of commodity-driven deforestation and associated carbon emissions.” *Nature Food* 7 (2): 138–151.

Sun, Liyang and Sarah Abraham. 2021. “Estimating Dynamic Treatment Effects in Event Studies with Heterogeneous Treatment Effects.” *Journal of Econometrics* 225 (2): 175–199. 10.1016/j.jeconom.2020.09.006.

Trase. 2025. “Brazil slaughterhouses and other animal products facilities: Data sources and methods.” 10.48650/49YM-HZ10.

USDA Foreign Agricultural Service. 2026. “Production, Supply and Distribution Online: Livestock and Poultry.” https://apps.fas.usda.gov/psdonline/app/index.html. Data file of April 9, 2026, accessed October 5, 2026.

Valadares Filho, Sebastião de Campos, Pedro Veiga Rodrigues Paulino, Karla Alves Magalhães, Mário Fonseca Paulino, Edenio Detmann, Douglas dos Santos Pina, and José Augusto Gomes Azevêdo. 2006. “Tabelas de composição de alimentos e exigências nutricionais de zebuínos: dados brasileiros.” In *Anais do V Simpósio de Produção de Gado de Corte e I Simpósio Internacional de Produção de Gado de Corte*, pp. 47–80. Viçosa: Universidade Federal de Viçosa.

World Trade Organization. 2026. “World Trade in Agricultural Products in Charts.” https://data.wto.org/en/dataset/agcharts. Data file agriculture_trade_data_with_hscodes.xlsx, last modified 10 February 2026. Accessed on 2026-10-30.

zu Ermgassen, E. K. H. J., C. Suavet, H. Biddle, N. Su, Y. Prada Moro, V. Ribeiro, T. Carvalho, and M. J. Lathuillière. 2023. “Brazil beef supply chain (2010–2020) (Version 2.2) [Data set].” 10.48650/AYAA-HH56.

Appendix A Additional details for the feedlot detection approach

A.1 Imagery

Detection uses the WPM camera on CBERS-4A, distributed free by INPE as a pan-sharpened color product at 2 m. To my knowledge it is the only free imagery with national coverage that resolves individual pens; Sentinel-2 (10 m) and Landsat (30 m) do not. Of the 4,115 scenes acquired over Brazil in 2024 I keep one per tile (1,089 tiles), preferring dry-season

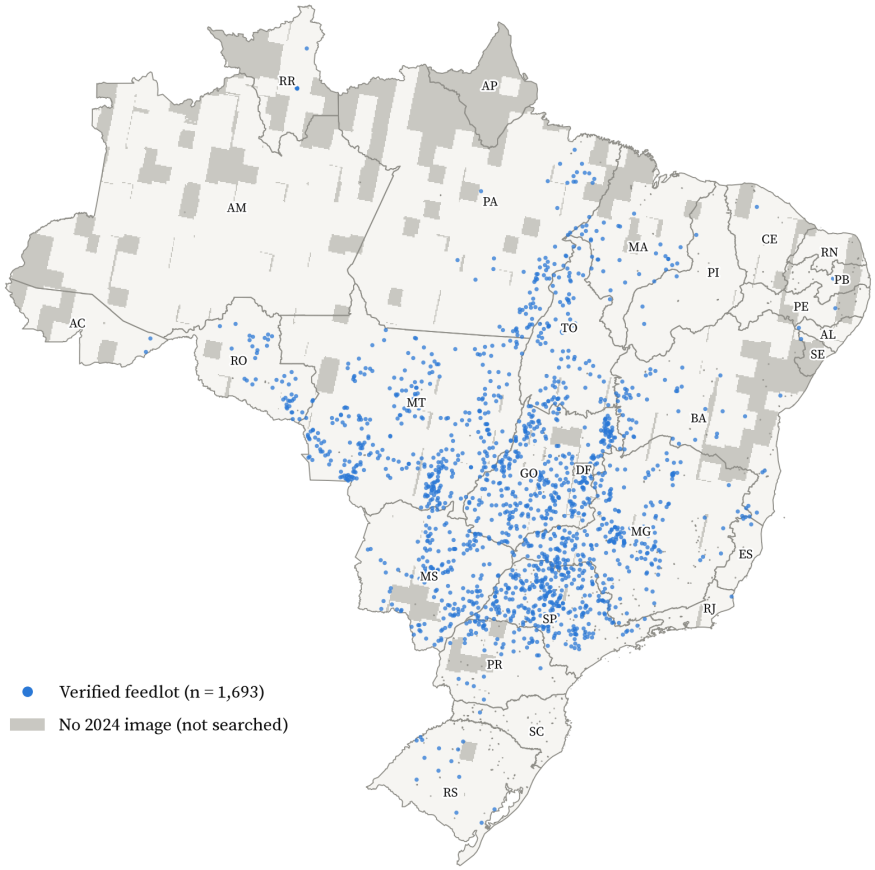


FIGURE A1. Verified feedlots and 2024 image coverage

Notes: Blue dots mark the 1,693 verified feedlots. Gray areas are the 118 image tiles that CBERS-4A did not acquire in 2024. They cover 14% of Brazil's area and were not searched. Labels are state abbreviations.

dates and scenes with the least missing data. The satellite did not acquire 118 tiles in 2024, so 14% of Brazil's area was never searched (Figure A1). For opening-year estimation, I use Landsat 5, 7, 8 and 9 surface reflectance (Collection 2), the only archive long enough. For each facility I take every scene with under 80% cloud cover from 1995 to mid-2026 over a 3 km window and mask cloud and shadow pixel by pixel. The median facility has 740 usable observations and a pen footprint of 5.4 ha, about 60 Landsat pixels.

A.2 Detector and training data

I trained a single-stage convolutional neural network classifier using the medium-sized YOLOv11 ("You Only Look Once") architecture with one class (a pen block). I use a "warm start" approach where I initialize the model using weights that Aires, Martins, Hester et al. (2026) trained imagery of U.S. feedlots. An earlier whole-image classifier (ResNet-18) I trialed had near-zero precision nationally despite a test AUC of 0.997; localizing pens using

the YOLO architecture and training on realistic negatives resolved this problem.

Positive examples are 1 km chips with every visible pen block outlined by hand. The starting set came from Google Places searches for *confinamento* terms on a national grid: 424 listings, of which I confirmed 215 as feedlots in Google Earth. Negative examples are random points within 15 MapBiomas land-cover classes across Brazil and "hard negatives", the model's own confident false positives from earlier rounds. The final training set has 1,125 facilities (1,386 boxes) and 1,789 negative chips, split 80/10/10 into training, validation and test sets by municipality.

A.3 National search, review and regional balance

The model scans every scene in overlapping 1 km windows (Figure A2). In the final round it returns 30,833 boxes with confidence of at least 0.2. Boxes within 500 m edge-to-edge are merged into one facility, the rule that also defines a facility in the registry, giving 21,864 candidates; 20,469 remain after removing those outside Brazil and those whose pens were all already labeled. Of these, 20,069 are at places with no known facility and 400 are at known facilities with unlabeled pens. I reviewed candidates in descending order of confidence on an 800 m crop of the 2 m image, with a link to Google Earth, and recorded yes, maybe or no. Only "yes" enters the registry. Outlining the pens of each accepted site served as a second inspection. I did all the review myself.

I iterated through five rounds of this procedure. In round 5 I reviewed every candidate with confidence of at least 0.4 and stopped below that once the confirmation rate had fallen to about 3%. To limit regional bias, hard negatives were drawn with weights inversely related to each state's count in round 4 and tilted toward the states with the highest false-positive rates in round 5. Review queues were interleaved by region in rounds 3 and 4 and cut at a national confidence threshold in round 5, so low-yield regions were reviewed as deeply as high-yield ones (Table A1).

A.4 Detection accuracy

On the held-out municipalities (111 facilities, 308 negative chips) the final model has precision 0.96 and facility recall 0.87 at a confidence threshold of 0.5, and 0.91 and 0.91 at 0.2 (Figure A3). The facility-level F1 for the final model is 0.915 at the 0.5 confidence threshold. Most of these negatives are mined false positives from earlier review rounds. Nationally, only 7% of reviewed round-5 candidates were confirmed, which is why every facility is verified by eye. This is largely due to the known problem of "class imbalance" in machine learning. In this context, since feedlots are so unlikely to be present on any given pixel imaged throughout Brazil, even with very high precision on the test sample, many false positives are generated by the model on country-wide inference passes, especially at

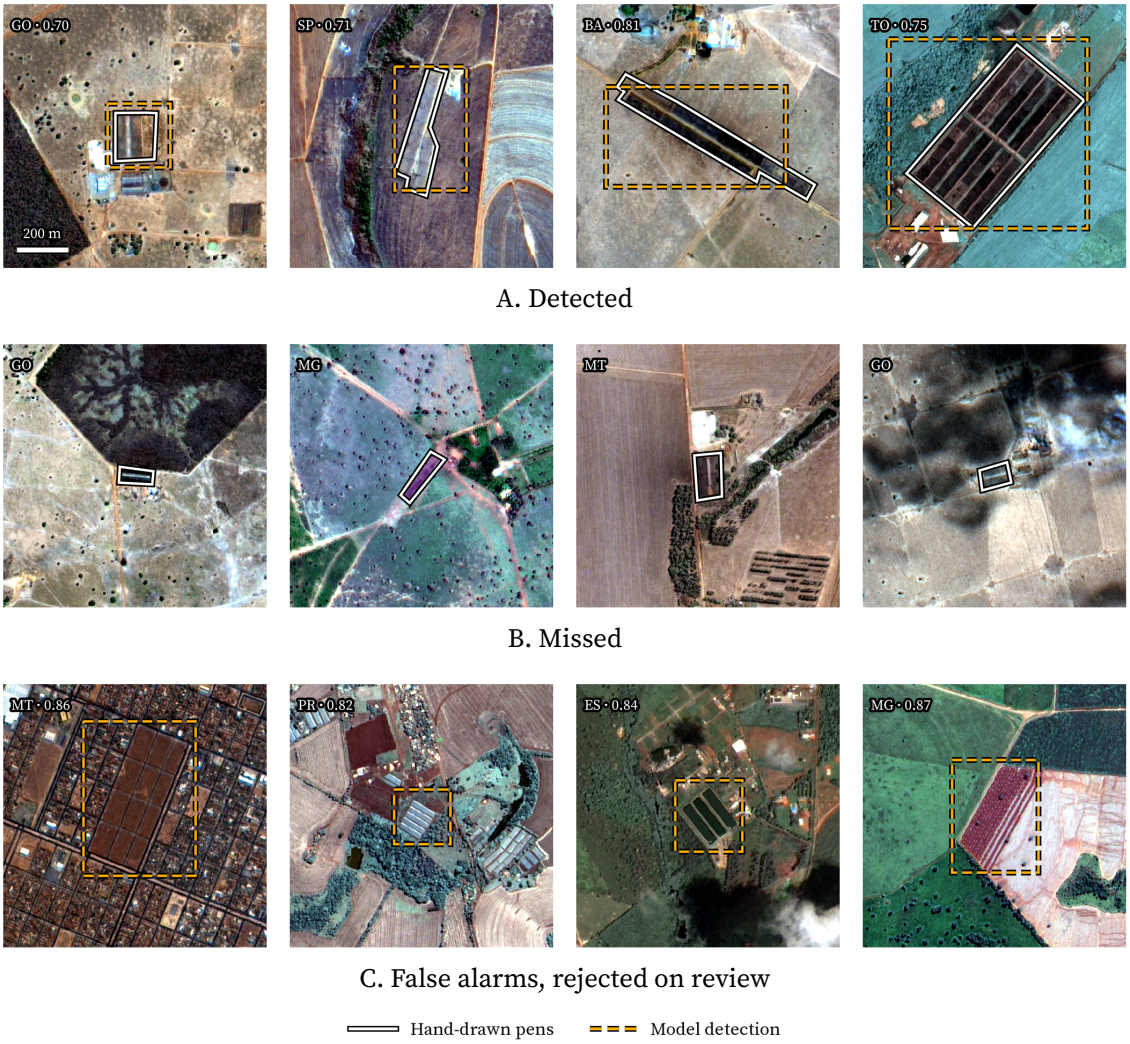


FIGURE A2. Model detections, missed facilities, and rejected candidates

Notes: Each tile is a 1 km chip of the 2-meter imagery. Solid white outlines are pens I outlined by hand and dashed orange boxes are model detections. Labels give the state and, where the model made a detection, its confidence. The white bar in the first tile marks 200 meters. Panel A shows facilities the model detected, Panel B shows labeled facilities it missed, and Panel C shows detections I rejected on review.

TABLE A1. Regional balance of the search and review

Region	Verified facilities		Round 5 national search		
	After rounds 1–2	Final registry	Candidates	Reviewed (%)	Confirmed (%)
Center-West	118	811	7,079	48	8.4
Southeast	87	520	4,865	40	7.8
North	40	210	2,161	39	8.1
Northeast	5	92	2,428	44	4.2
South	6	60	3,536	39	1.6

Notes: The first two columns count the verified facilities in the registry after rounds 1 and 2 and after round 5. Candidates are the 20,069 round 5 candidates at places with no known facility. Reviewed is the share of candidates I inspected, and Confirmed is the share of reviewed candidates I accepted as feedlots.

lower confidence levels.

Recall cannot be measured exactly, because no census of locations exists. Three benchmarks offer some context: the 87 to 91% recall metric on held-out chips, and two from the national search. There the model re-detects 82% of the facilities known before round 5 (70% in municipalities with no training example), rising from 70% for footprints under 3 ha to 92% above 15 ha. The national figures are lower than the chip test even for the same held-out facilities, probably because test chips are centered on the pens while the search tiles each scene blindly and relies on one 2024 image per tile.

A.5 Opening-year estimation

From each hand-drawn footprint I define three zones: the pens (A, eroded by 30 m to avoid mixed edge pixels), a 300 m ring holding the rest of the facility (B), and control land beyond it (C). For scene t and spectral index k the feature is a within-scene difference,

$$y_{it}^{k} = q_{\tau}\{x_k(p,t) : p \in A_i\} - \text{med}\{x_k(p,t) : p \in C_i\}, \tag{A1}$$

where q_τ is a quantile over clear pixels. Any additive scene-level nuisance (sensor generation, atmosphere, sun angle) cancels exactly, so no cross-sensor harmonization is needed. The seven indices include NDVI, two bare-soil indices (BSI, NDBI) and tasseled-cap wetness.

Estimator 1 (site-level structural breaks). Within regime j each feature follows a level plus an annual harmonic,

$$y_{it}^{k} = \mu_{ij}^{k} + a_{ij}^{k}\cos(2\pi d_t/365.25) + b_{ij}^{k}\sin(2\pi d_t/365.25) + \varepsilon_{it}^{k}, \tag{A2}$$

with d_t the day of year. Break dates are common to six standardized features and estimated

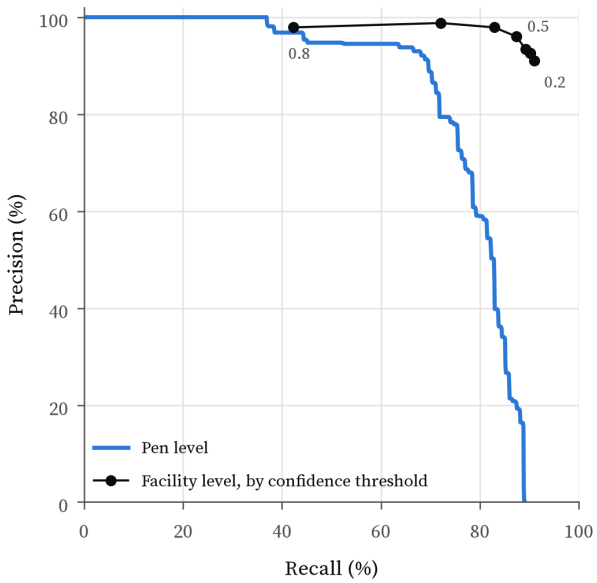


FIGURE A3. Precision and recall of the detector in held-out municipalities

Notes: Evaluated on the 111 facilities and 308 negative chips in municipalities held out from training. The blue line traces precision and recall for individual pen blocks as the confidence threshold varies. Black markers show precision and recall for facilities at confidence thresholds from 0.8 (left) to 0.2 (right).

by least squares (Bai and Perron 1998), with at most four breaks. A logistic regression then scores how feedlot-like each regime is from its fitted levels and seasonal amplitudes. It is trained only on each site's own endpoints, 1995 to 1997 as "not a feedlot" and its latest years as "feedlot", pooled across sites. Because the feedlots are verified to still exist in 2024, the scores are projected onto a non-decreasing sequence by isotonic regression, and the break chosen as the opening estimate is the start of the regime with the largest remaining rise.

Estimator 2 (pixel-level). For up to 120 pen pixels and three indices with a known expected sign (NDBI up, NDVI down, BSI up), I fit the same model with a single break, discard breaks of the wrong sign, and take the mode of a strength-weighted vote across pixels.

Combination. The estimate is the later of the two dates. Both estimators have an early-biased tail and are only moderately correlated (0.59), so taking the later date corrects the bias where they disagree, which a constant shift cannot do. They agree within one year for 66% of facilities. Surface temperature, a fused-LASSO segmentation and published cross-sensor coefficients were tested and did not help.

TABLE A2. Opening-year accuracy, exactly dated facilities

	Holdout sites	Development sites	All sites
Facilities	42	64	106
Exact year (%)	45	25	33
Within ±1 year (%)	74	52	60
	(59–85)	(40–63)	(51–69)
Within ±2 years (%)	88	61	72
	(75–95)	(49–72)	(63–79)
Mean error (years)	−0.5	0.0	−0.2
Mean absolute error (years)	1.2	2.9	2.2
Operating status correct (%)	95.2	88.6	91.2

Notes: The sample is the facilities whose opening I could date to an exact year in Google Earth's historical imagery. The holdout sites were set aside before labeling. The development sites are the other labeled facilities, which I used to tune the estimator. Error is the estimated minus the true opening year. 95% intervals are in parentheses. Operating status is whether a facility is operating in a given year, and it is evaluated over all facility-years from 2000 to 2024.

A.6 Validation of Opening Years

I sampled 300 of the facilities then in the registry, stratified by region (with floors of 25 for the Northeast and South), footprint size and a prior before/after-2010 classification, and assigned 100 to a holdout before labeling. For each I recorded the last Google Earth image without pens and the first with them. Of 300 usable labels, 106 are exact (consecutive years), 164 are intervals and 30 were already operating in the earliest image. I tuned the estimator on the other labeled sites and did not use the holdout for tuning. The estimates evaluated in Table A2 are the ones used in the paper. They come from the estimator run on all 1,693 sites, observing through 2026 with break dates capped at 2024, which gives late openings some post-break data.

The development sites score lower than the holdout although they were used for tuning, so I report both and take the pooled column as the conservative summary. Where the two estimators agree, 68% of estimates are within one year and 82% within two; where they disagree, 40% and 47%. The dating errors are not classical. Estimates are compressed toward the middle of the window: the mean error is +2.5 years for openings in 2012 or earlier (13 facilities), +2.0 for 2013 to 2017 (24), between −1.0 and −1.7 for 2018–23 (59) and −2.2 for 2024 (10). By region, the share within one year is 59% in the Center-West (39 facilities), 67% in the Southeast (30), 60% in the North (15), 38% in the Northeast (13) and 78% in the South (9).

Appendix B Additional event study results

Figure A4 repeats the main event study with the interaction-weighted estimator of Sun and Abraham (2021), with municipality and year fixed effects. In the main sample, this estimator uses the municipalities first exposed in 2024 as the comparison group for every cohort. The average effect over years 0 to 12 is 0.20 feedlots per 100,000 head (standard error 0.06), compared with 0.27 in the main specification.

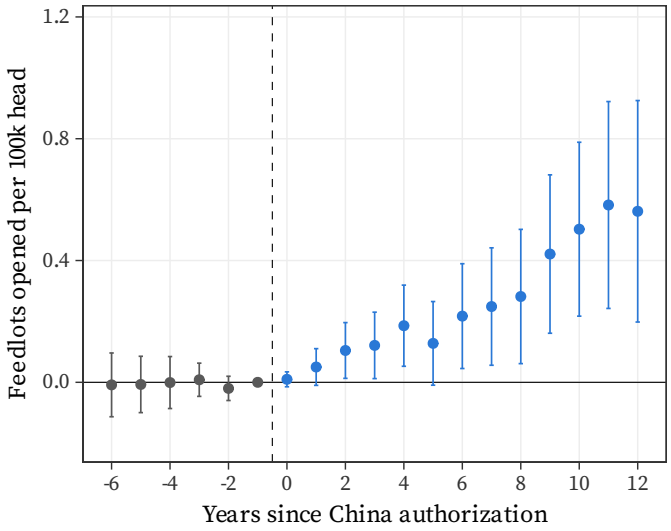
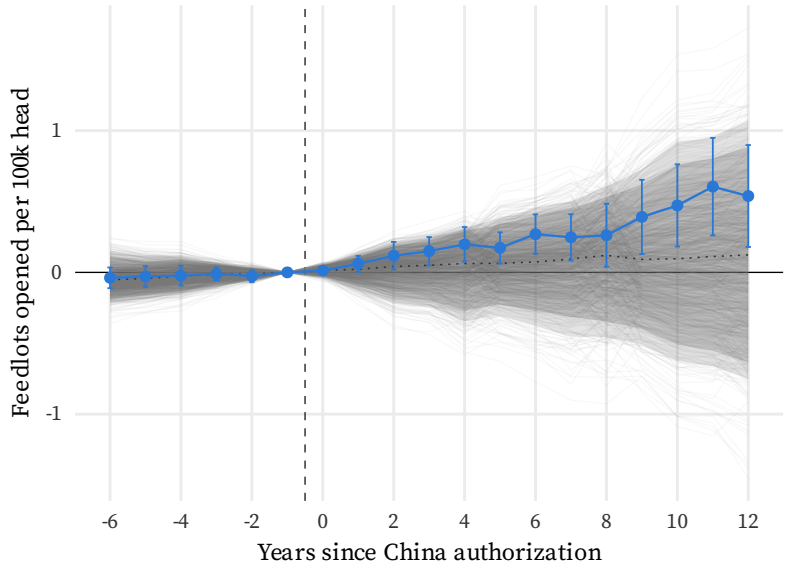


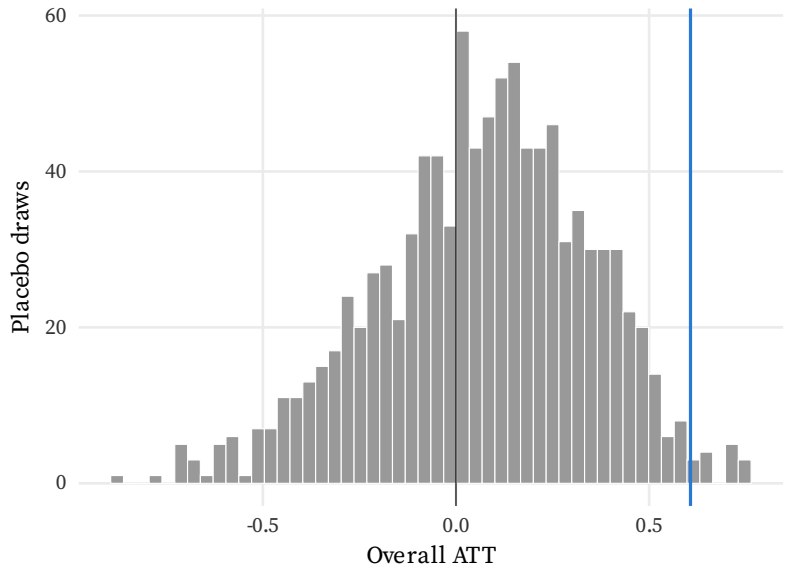
FIGURE A4. Event-study estimates with the Sun and Abraham estimator

Notes: The figure shows event-study estimates from the estimator of Sun and Abraham (2021) with municipality and year fixed effects, relative to the year before exposure. The outcome, the definition of exposure, and the sample of 1,628 municipalities are the same as in Figure 8A. Bars are pointwise 95% confidence intervals from standard errors clustered by immediate geographic region.

Figure A5 shows the results of the timing placebo described in Section 4.4.



A. Actual and placebo event-study paths



B. Average effect after exposure

FIGURE A5. Event-study estimates under randomly reassigned authorization dates

Notes: Each placebo draw randomly reassigns the authorization years across the 67 plants, holding the number of plants in each wave fixed, recomputes each municipality's year of first exposure, and re-estimates the main specification in Figure 8A. There are 1,000 draws. In Panel A, the thin gray lines are the placebo paths, the shaded bands cover the 5th to 95th and the 2.5th to 97.5th percentiles of the placebo estimates in each year, and the dotted line is their median. The blue line is the actual estimate with its 95% confidence interval. Panel B shows the distribution across placebo draws of the average effect over all years after exposure (0 to 18). The blue vertical line marks the actual estimate.

Appendix C Additional recentering details and results

C.1 Construction of recentered exposure

This appendix lists the steps behind the recentered exposure design of Section 4.5.

1. Fix the set of 73 candidate plants and assign each plant p to its nomination queue $q(p)$: the 15 plants nominated in the mid-2000s, or the 58 plants that were candidates from 2019 onward. Record the authorization year a_p of each plant, with $a_p = \infty$ for the six plants not authorized by 2024.
2. Compute the access of each municipality i to each plant p,

$$w_{ip} = \frac{\sum_{j \in i} s_j \, \kappa(d_{jp})}{\sum_{j \in i} s_j}, \qquad \kappa(d) = 2^{-d/69},$$

   where j indexes the rural properties in municipality i, s_j is the area of property j, and d_{jp} is the road distance in kilometers from property j to plant p.
3. Compute China's beef imports from all countries other than Brazil, D_t, for 2005 to 2024, and the shock to each plant, $c(a_p) = \sum_{t=a_p}^{2024} D_t$, with $c(\infty) = 0$.
4. Compute realized exposure, $C_i = \sum_p w_{ip} \, c(a_p)$.
5. Draw alternative assignments. For $s = 1, \ldots, 10{,}000$, permute the authorization years among the plants within each queue to obtain $a_p^{(s)}$, and compute $C_i^{(s)} = \sum_p w_{ip} \, c(a_p^{(s)})$.
6. Compute expected exposure, the mean of $C_i^{(s)}$ across assignments. Under permutations within queues it has the exact form $\mu_i = \sum_p w_{ip} \, \bar{c}_{q(p)}$, where $\bar{c}_q$ is the mean of $c(a_p)$ among the plants in queue q, and I use this form.
7. Compute recentered exposure, $\tilde{C}_i = C_i - \mu_i$, and its counterpart for each draw, $\tilde{C}_i^{(s)} = C_i^{(s)} - \mu_i$.
8. Estimate equations (6), (7), and (8).
9. Test the null of no effect by randomization inference. Let r_i denote the residual of the outcome from the specification estimated without exposure, so that it is net of the controls and, in the controlled specifications, of expected exposure. Compute $T = \sum_i \tilde{C}_i \, r_i$ and $T^{(s)} = \sum_i \tilde{C}_i^{(s)} \, r_i$ for each draw, weighting by the baseline herd in the linear specifications. The p-value is the share of draws with $|T^{(s)}| \geq |T|$. The balance tests in Table A3 use the same procedure with r_i replaced by a predetermined characteristic.

C.2 Balance

Table A3 reports the balance tests discussed in Section 4.5. Panel A correlates recentered exposure with municipality characteristics determined before the first authorization. Panel B correlates the timing of a plant's authorization, measured as its shock minus the average shock in its queue, with characteristics of the plant.

TABLE A3. Balance of recentered exposure on predetermined characteristics

	Correlation	RI p-value
A. Municipalities: correlation with recentered exposure		
Latitude	0.026	0.87
Longitude	−0.043	0.73
Log land area	−0.052	0.51
Log cattle herd, 2000 to 2004	−0.007	0.92
Pasture share of land area, 2000 to 2004	0.031	0.83
Joint test of the five characteristics		0.86
Expected exposure, μ_i	0.324	0.34
B. Plants: correlation with the timing of authorization within the queue		
Owned by one of the three largest meatpackers	−0.020	0.85
Located in an Amazon frontier state	0.062	0.59
Latitude	0.028	0.81
Longitude	0.085	0.49
Slaughter capacity	0.130	0.30

Notes: Randomization inference (RI) p-values are the share of 10,000 permutations of authorization years within nomination queues that produce a correlation at least as large in absolute value. In Panel A, the sample is 5,563 municipalities, or 5,530 for the herd and the joint test. The joint test regresses recentered exposure on the five characteristics and compares the sum of squared fitted values with its distribution across the same permutations. In Panel B, the sample is the 73 candidate plants, or 72 for slaughter capacity, which is measured in ordered categories. The three largest meatpackers are JBS, Marfrig, and Minerva. Amazon frontier states are Acre, Mato Grosso, Pará, Rondônia, and Tocantins.

C.3 Alternative specifications

Table A4 reports alternative specifications for the estimates in Table 2. Panel A varies the controls in the preferred PPML specification. The first row repeats the estimate from the main text. The second row replaces the log herd control with an offset, which fixes the coefficient on the log herd at one and so models feedlot growth per head of cattle. The third row keeps the offset and drops the other controls. The fourth row adds the number and pen area of feedlots in 2004 to the baseline controls. I do not include these two variables in the main specification because I observe only the feedlots that operate in 2024, so the 2004 stock is measured among facilities that survived, and survival may itself respond to exposure. The last two rows drop the herd control. Panel B reports the linear specifications with the outcome in levels, without scaling or weighting by the herd.

TABLE A4. Alternative specifications of the recentered exposure design

	Number of feedlots			Pen area (hectares)		
	Estimate	SE	RI p-value	Estimate	SE	RI p-value
A. PPML controlling for expected exposure						
Baseline controls	0.207	0.042	0.023	0.194	0.052	0.047
Herd as an offset	0.199	0.041	0.026	0.190	0.051	0.051
Herd as an offset, no other controls	0.195	0.041	0.022	0.188	0.057	0.058
Baseline controls and 2004 feedlot stock	0.184	0.038	0.032	0.176	0.050	0.058
Geography controls only	0.217	0.077	0.194	0.202	0.094	0.259
B. Linear specifications, outcome in levels						
OLS	0.018	0.006		0.186	0.056	
Recentered IV	0.043	0.016	0.049	0.371	0.159	0.121
Controlled OLS	0.103	0.039	0.142	0.834	0.452	0.279

Notes: Each row reports the coefficient on cumulative exposure to Chinese demand, in Mt-years, for the change from 2004 to 2024 in the number of feedlots and in their pen area. Panel A estimates equation (8) under alternative sets of controls. Baseline controls are latitude, longitude, log land area, the log of the 2000 to 2004 cattle herd, and the 2000 to 2004 pasture share. The herd offset enters the log herd with a coefficient of one in place of the log herd control. The 2004 feedlot stock is the number and pen area of the feedlots operating in 2024 that had opened by 2004. Geography controls are latitude, longitude, and log land area. Panel B estimates equations (6) and (7), and OLS without adjustment, with the outcome in levels, the baseline controls, and no weights. Standard errors (SE) allow for spatial correlation within 300 km (Conley 1999). Randomization inference (RI) p-values for the null of no effect are from 10,000 permutations of authorization years within nomination queues.

Appendix D Land-Use Counterfactual: Implementation

This appendix documents the implementation of the counterfactual exercise in Section 5. For each step, I describe the data and parameters used, what the step produces, and the choices I made where more than one reasonable implementation was available. Table A5 lists each object along with its source and the value used in the central estimate.

D.1 Steps and parameters

Let f index municipalities in their role as feedlot locations and i index municipalities in their role as suppliers of cattle. The terminal year of the exercise is 2024, which is the last year of both the feedlot data and the exposure measure. Land cover is observed through 2023, the last year available in the MapBiomas series, so pasture area, the land remaining in each cover class, and historical land-cover transitions all refer to 2023. The exercise proceeds from the pen area that municipality f added between 2004 and 2024, P_f, through the attributable share s_f from equation (10), the conversion factor $\kappa_{s(f)}$ from pen area to cattle finished per year, which varies with the state $s(f)$ of the feedlot municipality, the sourcing weights ω_{if}, and the pasture requirement per head from equation (9) divided by twelve times the stocking density s_i. The additional pasture required in supplying municipality i is therefore

$$\Delta L_i = \sum_f \omega_{if}\, \kappa_{s(f)}\, s_f P_f\, \frac{r^w A^P - A^F}{12\, s_i}. \tag{A3}$$

Summing ΔL_i across municipalities gives the national pasture requirement, and the land-cover and carbon steps are applied to each ΔL_i separately. Apart from the stocking density s_i and the state rate $\kappa_{s(f)}$, the parameters in equation (A3) are national. The spatial pattern of the results is therefore determined by where the attributable pen area is located, the throughput of feedlots in that state, where those feedlots source their cattle, and the stocking density and land-cover history of the supplying municipalities.

D.2 Attributable pen area and cattle

Pen area is measured as the detected area of every feedlot site standing in 2024, dated by the year in which the site first appears in the imagery and aggregated to the municipality level. In 2024, 779 municipalities have positive pen area, totaling 14,935 hectares. Sites dating from 2004 or earlier account for 177 hectares in 18 municipalities, so 14,759 hectares were added over the sample period. The attributable share s_f applies β to each municipality's cumulative exposure. Across municipalities with feedlots, the median share is 0.65; the share exceeds 0.9 in 22% of these municipalities and falls below 0.1 in 14%. Applying these

TABLE A5. Objects and parameters of the land-use counterfactual

Object	What it is	Source	Value or rule
β	Semi-elasticity of pen area added 2004 to 2024 with respect to exposure	Table 2, Column 5	0.194 per Mt-year; alternatives 0.176 to 0.207 (Appendix C)
C_f	Cumulative exposure, 2005 to 2024	Section 4.5	0 to 36 Mt-years among municipalities with feedlots
P_f, $s_f P_f$	Pen area added 2004 to 2024 and its attributable part	Feedlot panel (Section 2.2); equation (10)	14,759 ha added in 779 municipalities; 8,794 ha attributable
H_t	Cattle finished in confinement nationally	dsm-firmenich census 2015 to 2024; Athenagro/ABIEC series 2003 to 2014 spliced to the census level	3.23 M in 2004, 7.96 M in 2024
κ_s	Cattle finished per hectare of pen per year, by state	$(H_{2024} - H_{2004})$ over pen area added, scaled by the state's 2024 throughput relative to the five census states	321 head per ha nationally; GO 272, MS 310, MT 317, MG 335, SP 386; 321 in other states
ω_{if}	Share of f's cattle supplied by i	Gravity model on transit permits, MT, PA, ES (Appendix D.3)	Origins in f's state; 2023 herd and pasture
d_{if}	Road distance from i to f	OpenStreetMap network	Hundreds of km; $\frac{2}{3}\sqrt{\text{area}/\pi}$ within a municipality
A^F	Age at feedlot entry, months	2023 nutritionist survey, bulls (Monsalve and Millen 2025)	22.6
A^P	Slaughter age of pasture-finished males, months	Transit permits, slaughter shipments from municipalities without feedlots (Appendix D.5)	30.4; oldest bracket at 45 months (42, 54)
w^F	Carcass weight of feedlot males, kg	Cargill feedlot benchmarking survey, 2023 (Appendix D.4)	305.9
w^P	Carcass weight of other males, kg	IBGE slaughter survey, 2023, residual	291.3; r^w = 1.05 (1.025 to 1.16)
s_i	Stocking density, head per hectare of pasture	IBGE herd over MapBiomas pasture, 2020 to 2023	Municipal, winsorized at 1 percent; feedlot municipalities take their microregion's value without feedlots
π_{ic}	Share of i's new pasture drawn from cover class c	MapBiomas transitions into pasture, 2004 to 2023	Municipal; allocation capped by the land of class c remaining in 2023
$\bar{C}_{cb}$, C^P_b	Carbon stock per hectare of class c and of pasture in biome b	Fourth National Inventory, aggregated to MapBiomas classes (SEEG 2024) (Appendix D.7)	Biomass, litter, and dead wood; Amazon forest 165 t C, Cerrado savanna 41, pasture 8 to 10
Ration	Feed dry matter per feedlot animal and its composition	2023 nutritionist survey (Appendix D.8)	1.14 t; maize grain 54%, maize silage 8.8%, soybean meal 1.8%
Yields	Maize and soybean, tonnes per hectare	IBGE, national means 2022 to 2024	5.52 and 3.18; maize silage 10.7 t of dry matter

Notes: Each row gives the object as used in the central estimate. Mt-years are megatonnes of Chinese beef imports from countries other than Brazil, summed over the years a plant is authorized, as defined in Section 4.5.

shares to the pen area added yields 8,794 hectares attributable to exposure, or 60% of the total.

To convert pen area into cattle, I use the national count of cattle finished in confinement, which the dsm-firmenich industry census reports for 2015 to 2024 and the Athenagro series published by ABIEC reports for earlier years. The two series overlap between 2015 and 2019 and differ in level by approximately 9%. I therefore rescale the earlier series to the census level using the ratio of the two in the overlap years and use the rescaled values for 2003 to 2014. Between 2004 and 2024, the national count rose from 3.23 to 7.96 million head, while detected pen area rose by 14,759 hectares, which implies a marginal rate of 321 head per hectare per year. I use this marginal rate rather than the 2024 average of 533 head per hectare because the attributable capacity is a share of the capacity added over the period, and the census grew more quickly than the detected footprint over that period.

The census also reports state totals for the five largest feedlot states, and these show that throughput per hectare of detected pen area differs across states. In 2024, the state totals imply 581 head per hectare in São Paulo, 504 in Minas Gerais, 477 in Mato Grosso, 467 in Mato Grosso do Sul, and 410 in Goiás, against the national average of 533. I use this variation to let the marginal rate differ by state. For each of the five states, I multiply the national marginal rate by the state's ratio to the national average, which runs from 1.09 for São Paulo to 0.77 for Goiás, divided by the pen-area-weighted mean of the five ratios, 0.91. The normalization means that the five states keep their relative throughput while reproducing the national marginal rate when their rates are applied to the pen area each state added, so that the state rates and the national rate imply the same total growth in confined cattle. The resulting rates are 386 head per hectare in São Paulo, 335 in Minas Gerais, 317 in Mato Grosso, 310 in Mato Grosso do Sul, and 272 in Goiás. The remaining states, which have no published census total and account for 20% of the pen area added, receive the national rate. Applying the state rates to the attributable pen area yields 2.87 million head, which corresponds to 61% of the growth in confined cattle since 2004 and 36% of the 2024 total. Applying the national rate in every state instead gives 2.82 million head and changes the pasture requirement by less than 1%, since the state rates mainly shift cattle from Goiás toward São Paulo (Appendix D.9).

D.3 Sourcing network

The allocation of attributable cattle from feedlot municipalities to the municipalities that supply them is based on animal transit permits (GTA), which accompany cattle shipments in Brazil. These permits are issued by state animal-health agencies, and three states publish shipment-level records: Mato Grosso for 2021 to 2023, Pará for 2022 to 2023, and Espírito Santo for 2025. Each record reports the origin and destination municipality,

the stated purpose of the shipment, the sex and age bracket of the animals, and the number of head. I retain shipments of male cattle whose purpose is finishing (*engorda*) into municipalities with detected pen area in 2024 and collapse the records to the origin-destination-year level, which yields 25.5 million head, 19.8 million of them in Mato Grosso. Two features of the Pará data require a judgment call. In 2022, the purpose category combines rearing and finishing, and I treat shipments in this category as finishing. In addition, the female counts for 2022 cannot be recovered from the published workbook, which does not affect the analysis because only male shipments enter the sample.

Because each agency records the shipments that originate within its own state, the set of potential origins for a given feedlot municipality consists of the municipalities in its state. For each destination and year, I construct a cell for every origin in the state, including origins that shipped no cattle to that destination, and estimate

$$E[G_{ift}] = \exp\left(\delta_{ft} + \alpha \log B_{it} + \psi \log A^{P}_{it} - \tau\, d_{if} + \theta\, \mathbf{1}[i = f]\right) \tag{A4}$$

by Poisson pseudo-maximum likelihood, where G_{ift} is the number of head shipped from i to f in year t, B_{it} is the cattle herd of the origin municipality, A^{P}_{it} is its pasture area, d_{if} is road distance measured in hundreds of kilometers, and δ_{ft} is a destination-by-year fixed effect that absorbs the total number of cattle purchased by the feedlot municipality in that year. Herd and pasture area are measured in the year of the shipment, except that the 2025 shipments from Espírito Santo are paired with 2023 values, the last year for which pasture area is available. I compute road distance on the OpenStreetMap road network from the interior point of each origin municipality to the pen-area-weighted location of the feedlots in the destination municipality. Within a municipality, I use the internal distance $\frac{2}{3}\sqrt{\text{area}/\pi}$. For the 140 origin municipalities that the connected road network does not reach, which are located in areas served only by ferry, I add the straight-line distance to the nearest point on the network to the road distance from that point. The resulting estimation sample contains 49,737 cells covering 353 destination-years, of which 28% have a positive flow.

The estimated coefficients are $\widehat{\alpha} = 0.60$, $\widehat{\psi} = 0.26$, $\widehat{\tau} = 0.39$ per 100 km, and $\widehat{\theta} = 2.30$. The own-municipality indicator is not part of the standard gravity specification. I include it because distance alone substantially understates the extent to which feedlots source cattle locally: without the indicator, the model predicts that 15% of a Mato Grosso feedlot municipality's cattle originate in the municipality itself, compared with an observed share of 42%, whereas with the indicator the fitted share is 39%. The fit is weaker in the two smaller states. The fitted own-municipality share is 53% in Pará, compared with an observed share of 42%, and 44% in Espírito Santo, compared with 29%, and the model understates the long shipping distances observed in Pará, where the state-specific distance coefficient is close to zero. Since only these three states publish permit records, I apply

the pooled coefficients to every feedlot municipality in Brazil. The sourcing weights are then

$$\widehat{\omega}_{if} = \frac{\widehat{g}_{if}}{\sum_j \widehat{g}_{jf}}, \qquad \widehat{g}_{if} = \exp\left(\widehat{\alpha}\log B_i + \widehat{\psi}\log A_i^P - \widehat{\tau}\, d_{if} + \widehat{\theta}\,\mathbf{1}[i = f]\right), \tag{A5}$$

where herd and pasture area are measured in 2023, the sum runs over the municipalities in the state of f, and the fixed effect cancels in the normalization. Weighted by pen area, the predicted sourcing pattern draws 26% of a feedlot's cattle from its own municipality, 33% from origins within 100 km, and 11% from origins beyond 500 km, with a mean distance of 234 km, which is broadly consistent with the shipment distances documented in Section 3. Road distances were computed from the 760 municipalities with detected pen area in 2023. The 19 municipalities whose pen area first appears in 2024 therefore have no distance records, and the 0.25% of attributable cattle located in these municipalities is not allocated upstream.

D.4 Carcass weight ratio

The carcass ratio r^w compares beef output per animal across the two finishing systems. Because no national statistic reports carcass weight by finishing system, I combine a representative feedlot figure with the national average carcass weight for male cattle. The feedlot figure comes from the Cargill benchmarking survey of its feedlot clients for 2023, which covers 267 feedlots and 2.07 million head, or approximately 30% of the cattle finished in confinement in Brazil that year, 88% of which were male. The survey reports an entry weight of 376 kg live, an average daily gain of 1.55 kg over 112 days on feed, and a dressing percentage of 55.7, which together imply $w^F = 305.9$ kg of carcass, or 20.4 arrobas in the industry unit of 15 kg. The IBGE quarterly slaughter survey reports 19.9 million male cattle slaughtered under inspection in 2023, with an average carcass weight of 296.1 kg. Assuming that 90% of the 7.17 million cattle confined in 2023 were male, feedlot-finished cattle represent 32% of male slaughter, and the head-weighted identity

$$\bar{w} = \phi\, w^F + (1 - \phi)\, w^P \tag{A6}$$

implies $w^P = 291.3$ kg for the remaining male cattle and therefore $r^w = 1.05$.

Three features of this calibration are worth noting. First, it is restricted to male cattle. Cows average approximately 219 kg of carcass, so including them in the pasture-finished average would attribute the difference between cows and bulls to the finishing system. Second, the calibration is for 2023, which is the first year with both a representative feedlot carcass weight and a feedlot share of male slaughter large enough for the identity to be informative, and I apply the 2023 value to 2024. Third, the implied premium of 5% is modest. This reflects both the fact that the residual group includes semi-confined and

supplemented animals rather than only animals finished on extensive pasture, and the fact that pasture-finished male cattle in Brazil also reach relatively heavy carcass weights. The sensitivity range of 1.025 to 1.16 replaces the Cargill figure with the lighter carcass weight that the same survey reports for 2024 and with the heavier weight reported for a showcase tour of roughly ten feedlots organized by dsm-firmenich. The feedlot share ϕ has little effect on the result: varying the male share of confined cattle from 0.88 to 1 moves the premium from 4.9% to 5.2%.

D.5 Grazing ages

The age at feedlot entry is 22.58 months, the average initial age of bulls reported in the 2023 survey of Brazilian feedlot nutritionists by Monsalve and Millen (2025). The 36 respondents to that survey were responsible for 6.1 million animals, or roughly 80% of the cattle finished in confinement that year. Given 106 days on feed, the implied slaughter age of a feedlot-finished animal is approximately 26 months, which is below the 30-month limit imposed by China's import protocol. I do not estimate entry age from the transit permits because the finishing purpose category includes shipments for pasture fattening as well as feedlot entry; for example, 49% of the head shipped for finishing in Mato Grosso are 12 months old or younger. As a cross-check, however, the head-weighted mean age of finishing shipments into each feedlot municipality, averaged across municipalities using pen area as weights, is 16.5 months. The survey value is the more conservative choice, since a later entry age implies fewer grazing months saved per animal.

The slaughter age of pasture-finished cattle is calculated from transit permits for slaughter shipments (*abate*) of male cattle originating in municipalities with no detected pen area in 2024, pooled across the three states and weighted by head. The sample contains 2.5 million animals, with state-specific values of 29.0 months in Mato Grosso, 31.7 months in Pará, and 30.8 months in Espírito Santo, and a pooled value of 30.4 months. I use a single national value rather than municipal or regional values because municipal samples are sparse and because Mato Grosso alone spans three biomes. The permits report age in brackets, and I assign each bracket its midpoint: 2 and 8.5 months for the Mato Grosso brackets of 0 to 4 and 5 to 12 months, 6 months for the 0 to 12 month bracket used by the other two states, and 18.5 and 30.5 months for the 13 to 24 and 25 to 36 month brackets. The open bracket above 36 months requires an assumed value, and this choice matters for the result. The JBS slaughter records for 2018 to 2020 report dentition rather than age, and under the standard correspondence between permanent incisors and age, they imply an average age in this bracket of between 44 and 55 months, depending on the age assigned to animals with a full set of eight permanent incisors. I use 45 months in the central estimate and 42 and 54 months as sensitivity values, which move the pooled slaughter age to 29.7 and 32.5 months, respectively.

D.6 Stocking density

Stocking density is the municipality's cattle herd from the IBGE municipal livestock survey divided by its MapBiomas pasture area, pooled over 2020 to 2023 and winsorized at the first and ninety-ninth percentiles. Because cattle standing in feedlot pens are counted in the municipal herd but do not graze, municipalities with feedlots are assigned the pasture-weighted density of the municipalities without feedlots in their microregion. Of the feedlot municipalities, 723 receive their microregion value, 48 fall back to the mesoregion value because no municipality in their microregion is without feedlots, and the Federal District, which consists of a single municipality, receives the national value. The national pooled density over this window is 1.43 head per hectare. The substitution raises the pasture-weighted density of feedlot municipalities from 1.57 to 1.62 head per hectare, and it changes the final result by roughly 1%. Because the municipalities that supply feedlot cattle have above-average stocking densities, the 9.3 animal-months in equation (9) translate into 0.45 hectares per head rather than the 0.54 hectares implied by the national average density.

D.7 Land cover and carbon

Because stocking density is held fixed, the pasture requirement ΔL_i represents new pasture, and I determine its source using each municipality's own history of pasture expansion. From the MapBiomas annual maps, I tabulate for every municipality the area that transitioned into pasture between 2004 and 2023, by the cover class from which it came, restricting attention to classes with an inventory carbon value: forest formation (including flooded forest), savanna formation, mangrove, wetland, grassland, wooded restinga, planted forest, the annual and perennial crop classes, and the mosaic of agriculture and pasture. The shares π_{ic} are these areas normalized within each municipality. I allocate ΔL_i across classes in proportion to π_{ic}, subject to the constraint that the allocation to each class cannot exceed the area of that class remaining in the municipality in 2023. When a class is exhausted, the remainder is reallocated across the other classes in proportion to their shares. In the central estimate, this constraint reallocates 0.2% of the total requirement, and no municipality exhausts its eligible land.

Carbon stocks per hectare come from Brazil's Fourth National Greenhouse Gas Inventory, which reports the carbon stock of each vegetation type by biome and includes above-ground and below-ground biomass, litter, and dead wood. I use the aggregation of these values to MapBiomas classes published in the SEEG methodological documentation (SEEG 2024), which weights vegetation types by their share of each biome and distinguishes forest formation in the Cerrado by state. Each municipality is assigned the biome covering the largest share of its area, following IBGE's classification. The values

that matter most for the results are forest formation, at 165 tonnes of carbon per hectare in the Amazon, 122 in the Atlantic Forest, and between 62 and 99 across the Cerrado states; savanna formation, at 165 tonnes in the Amazon and 41 in the Cerrado; and pasture, at 10 tonnes in the Amazon and 7.6 in the Cerrado. Cropland and the mosaic class hold approximately 5 tonnes per hectare in the Cerrado, which is slightly less than pasture. The carbon stock loss in municipality i is

$$\Delta C_i = \sum_c \Delta A_{ic} \left(\bar{C}_{c,b(i)} - C^P_{b(i)} \right), \tag{A7}$$

that is, the area allocated to each class multiplied by the carbon stock of that class net of the pasture that replaces it, and I convert carbon to CO_2 using a factor of 44/12. Two omissions mean that this figure should be interpreted as a carbon stock at risk rather than as an emissions estimate. Soil carbon is excluded. In addition, the MapBiomas maps do not distinguish primary from secondary vegetation, so every hectare of forest or savanna is assigned the primary stock. The inventory assigns secondary vegetation 44% of the primary stock, so the figure overstates carbon losses in municipalities where historical pasture expansion has drawn on regrowth. In the central estimate, the converted land holds an average of 35.7 tonnes of carbon per hectare. Mosaic land and cropland account for 39% and 16% of the converted area, respectively, and release essentially no carbon, whereas forest formation accounts for 20% of the area and 73% of the carbon, and savanna accounts for 20% of the area and 23% of the carbon.

D.8 Feed-crop land

Feedlot-finished cattle consume crops that pasture-finished cattle do not, so part of the pasture saving from confined finishing is offset by the cropland required to produce feed. I compute this offset as a single national figure using the ration reported in the 2023 nutritionist survey and national average crop yields. The survey reports 106.2 days on feed and a dry matter intake of 10.75 kg per day for bulls, which implies 1.14 tonnes of dry matter per animal. Grain accounts for 54% of the diet, a figure I derive from the midpoints of the grain-share brackets reported in the survey, and I treat all of it as maize, which 92% of nutritionists identify as their primary grain. Roughage accounts for 15.7% of the diet, of which I assign 56% to maize silage, corresponding to the share of nutritionists who identify maize silage as their primary roughage; the remainder consists mostly of grass silage and sugarcane bagasse, to which I assign no cropland. Soybean meal accounts for 1.8% of the diet in the central case, which corresponds to a 5% inclusion rate in the rations that use it, weighted by the 36% of nutritionists who identify it as their primary or secondary protein source, and 5% in the upper case, which is its share in a published ration described as typical of feedlots in western Brazil. Byproducts such as cottonseed,

citrus pulp, and distillers' grain are assigned no land.

Yields are the IBGE national averages for 2022 to 2024: 5.52 tonnes per hectare for maize, which pools the first and second crops, and 3.18 tonnes per hectare for soybeans. Because maize silage yields are not published, I derive them from the grain yield. At 87.6% dry matter, the grain yield corresponds to 4.83 tonnes of dry matter per hectare, and dividing by a grain share of whole-plant dry matter of 0.45, the value reported in Brazilian field trials (Cruz 1998; Mello, Nörnberg, Rocha et al. 2005), gives 10.7 tonnes of silage dry matter per hectare. I convert soybean meal to soybeans using a crushing yield of 0.78 kg of meal per kg of beans and charge all of the soybean land to the meal rather than apportioning it between meal and oil. The dry matter contents of 87.6% for maize grain and 88.6% for soybean meal are taken from the Brazilian feed composition tables (Valadares Filho, Paulino, Magalhães et al. 2006). The resulting cropland requirement is 0.146 hectares per feedlot-finished animal, of which maize grain accounts for 0.128 hectares and silage and soybean meal for approximately 0.009 hectares each. For the 2.87 million attributable cattle, this amounts to 0.42 million hectares, or 33% of the pasture requirement, and 0.47 million hectares when soybean meal is set to 5% of the diet.

I report this figure alongside the pasture requirement rather than netting it against the map or the carbon total, for two reasons. First, feed crops are grown in the grain-producing regions, and a hectare of maize released in those regions does not necessarily avert a hectare of pasture conversion in a cattle-producing region. Second, a large share of Brazilian maize is grown as a second crop on soybean land following the soybean harvest, so the maize hectares computed here represent crop-hectares rather than land that would otherwise be idle, which makes 0.42 million hectares an upper bound on the land actually released. In any case, cropland and pasture hold similar carbon stocks under the inventory factors, so netting would have little effect on the carbon estimate.

D.9 Sensitivity

Figure A6 shows how the pasture requirement changes under alternative choices, holding all other parameters at their central values. The first four rows replace β with the alternative estimates reported in Appendix C: the coefficient from the same regression using the count of feedlots opened as the outcome, the specification with the herd included as an offset, the control set that adds the 2004 stock of feedlots, and the specification with geography controls only. These alternatives imply between 1.23 and 1.32 million hectares of additional pasture and between 160 and 174 million tonnes of CO_2. The count of feedlots produces nearly the same allocation as pen area because site size does not vary with exposure. The remaining rows vary the calibrated parameters. With no carcass premium, the requirement falls to 1.08 million hectares, which corresponds to the grazing-time saving alone, while a premium of 1.16 raises it to 1.75 million hectares. Assigning the oldest

age bracket 42 or 54 months yields 1.19 or 1.59 million hectares, respectively, and allowing feedlot municipalities to retain their own stocking density changes the result by 1.5%. Applying the national rate of 321 head per hectare in every state, in place of the state rates described in Appendix D.2, gives 1.28 million hectares and 171 million tonnes of CO_2; the state rates move land from Goiás toward São Paulo and change the national total by less than 1%. Beyond this, I do not vary the conversion from pen area to cattle, the sourcing weights, or the land-cover shares. I also do not propagate the sampling uncertainty of β through the accounting chain, since the chain combines several calibrated parameters and a confidence interval based on a single coefficient would overstate the precision of the overall estimate.

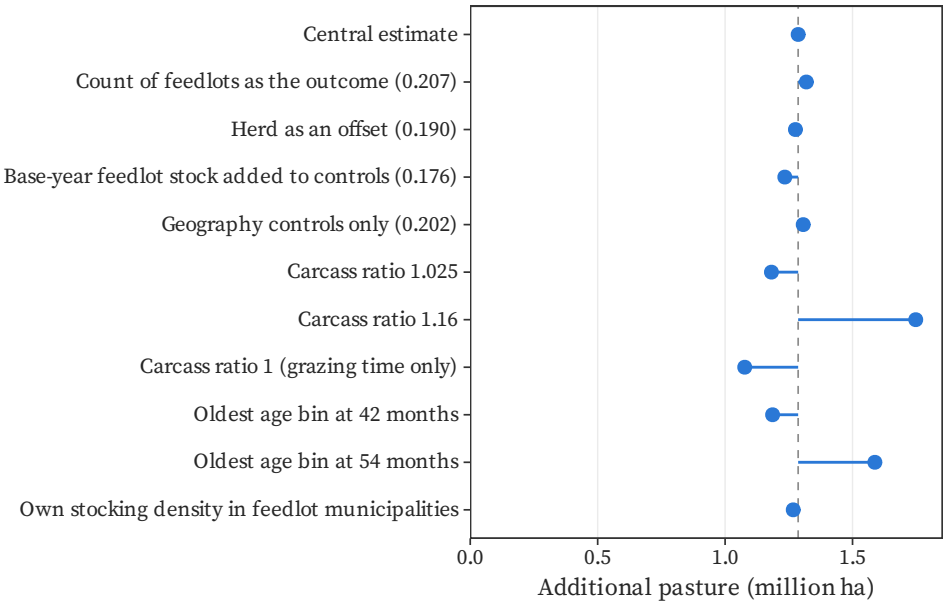


FIGURE A6. Sensitivity of the additional pasture requirement

Notes: Each point is the national additional pasture requirement under one change to the central calibration, which uses the pen-area estimate of β (0.194), a carcass ratio of 1.05, 45 months for the oldest age bracket, the state rates of cattle finished per hectare of pen, and the microregion stocking density for municipalities with feedlots. The dashed line marks the central estimate of 1.29 million hectares. The first four alternatives are the estimates of β in Appendix C, with the coefficient in parentheses.

Appendix E Additional details on the Brazilian beef industry

E.1 Feedlot production

Two surveys of feedlot nutritionists, whose clients accounted for 75% of the cattle finished in feedlots in 2019 and 80% in 2023, describe the animals and the feeding period (Silvestre and Millen 2021; Monsalve and Millen 2025). The typical animal is a Nelore bull. In 2023, 90% of the nutritionists' clients fed bulls and 84% fed Nelore cattle in particular. Cargill's benchmarking survey for the same year, which covers close to 30% of confined cattle, reports that 88% of the animals were male (Cargill 2024). Bulls entered the feedlot at 22.6 months and 385 kg on average, gained 1.59 kg per day over 106 days on feed, and left at 558 kg. The 2019 figures are nearly identical: 376 kg at entry, 1.58 kg per day, 107 days, and 556 kg at exit. Diets are grain based. Corn was the primary grain for 92% of nutritionists, roughage averaged 16% of dry matter and was most often corn silage, and 93% of clients fed agro-industrial coproducts such as citrus pulp, whole cottonseed, and distillers' grains. Pens provided 14 square meters per animal on average. Finally, most feedlot cattle are sold as a commodity rather than through a beef quality program, which was the case for 87% of clients in 2023.

Not all confined cattle belong to the feedlot operator. Under the arrangement known as "boitel", a rancher keeps ownership of the animals and pays the feedlot to finish them, with the charge set as a daily rate, a partnership share, the arrobas produced, or the dry matter consumed (Scot Consultoria 2024). Scot Consultoria describes the service as an alternative to the high investment required to start a feedlot, and at one Mato Grosso feedlot it profiles, 70% of the cattle on site belonged to third parties. In the census, boitel cattle made up between 18.5% and 23.3% of confined cattle in each year from 2020 to 2025 (dsm-firmenich 2025), and several of the twenty largest operators finish cattle for third parties (Revista DBO 2025). Confinement is also seasonal. Ranchers use boitels in part to relieve pastures in the dry season (Scot Consultoria 2024), and the census's monthly occupancy series rises from a trough in January and February to a peak in September and October (dsm-firmenich 2025). Because cattle are on feed for roughly 100 days, a feedlot can finish several times its static capacity in a year. For example, the Confinamento Monte Alegre in Barretos, São Paulo, has static capacity for 23,500 animals and finished 63,213 head in 2024, and the twenty largest operators together finished 2.46 million head that year, or roughly 30% of the census total (Revista DBO 2025).

E.2 Additional Figures

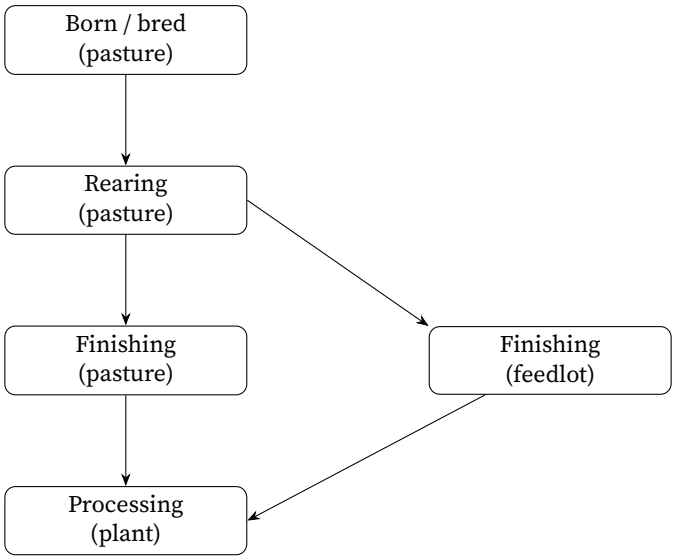


FIGURE A7. Stages of the cattle supply chain

Notes: Cattle are bred and reared on pasture. They are then finished either on pasture or in a feedlot before they are sent to a processing plant for slaughter.

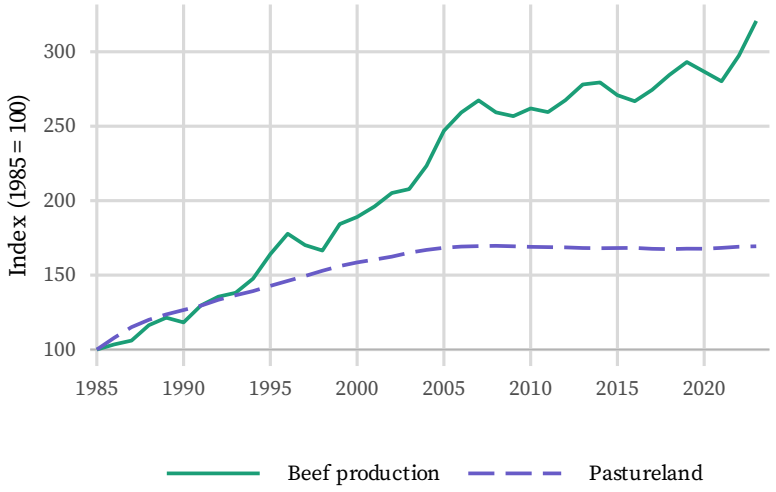


FIGURE A8. Beef production and pastureland in Brazil, 1985 to 2023

Notes: Both series are indexed to 100 in 1985. Beef production is the annual tonnage of cattle meat reported by FAOSTAT. Pastureland is the area classified as pasture in the MapBiomas land-cover maps.

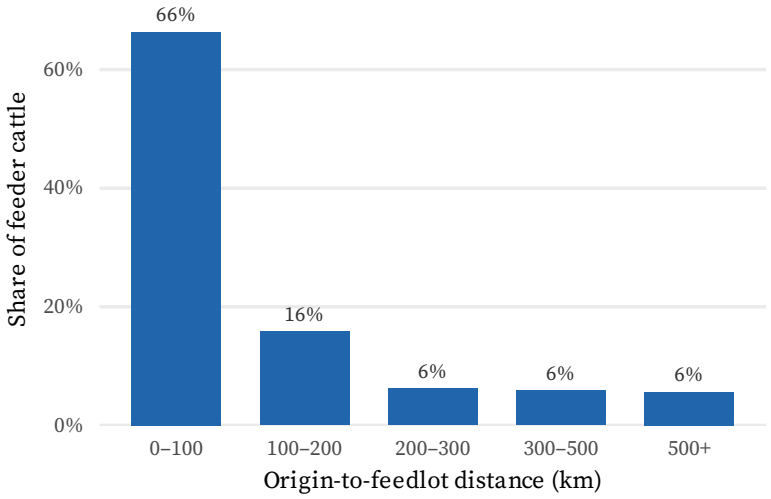


FIGURE A9. Distances cattle travel to feedlot municipalities

Notes: The figure shows the share of cattle shipped from Mato Grosso origins for finishing in municipalities with at least 5 hectares of feedlot pens, from 2013 to 2024, by straight-line distance between the origin and destination municipality centroids. Shipments are from animal transit permits (GTA).